HZB Helmholtz Zentrum Berlin

SwedNESS: Real-Space Neutron Imaging

Extreme Imaging
fast, large, high-resolution

Nikolay Kardjilov

Introduction

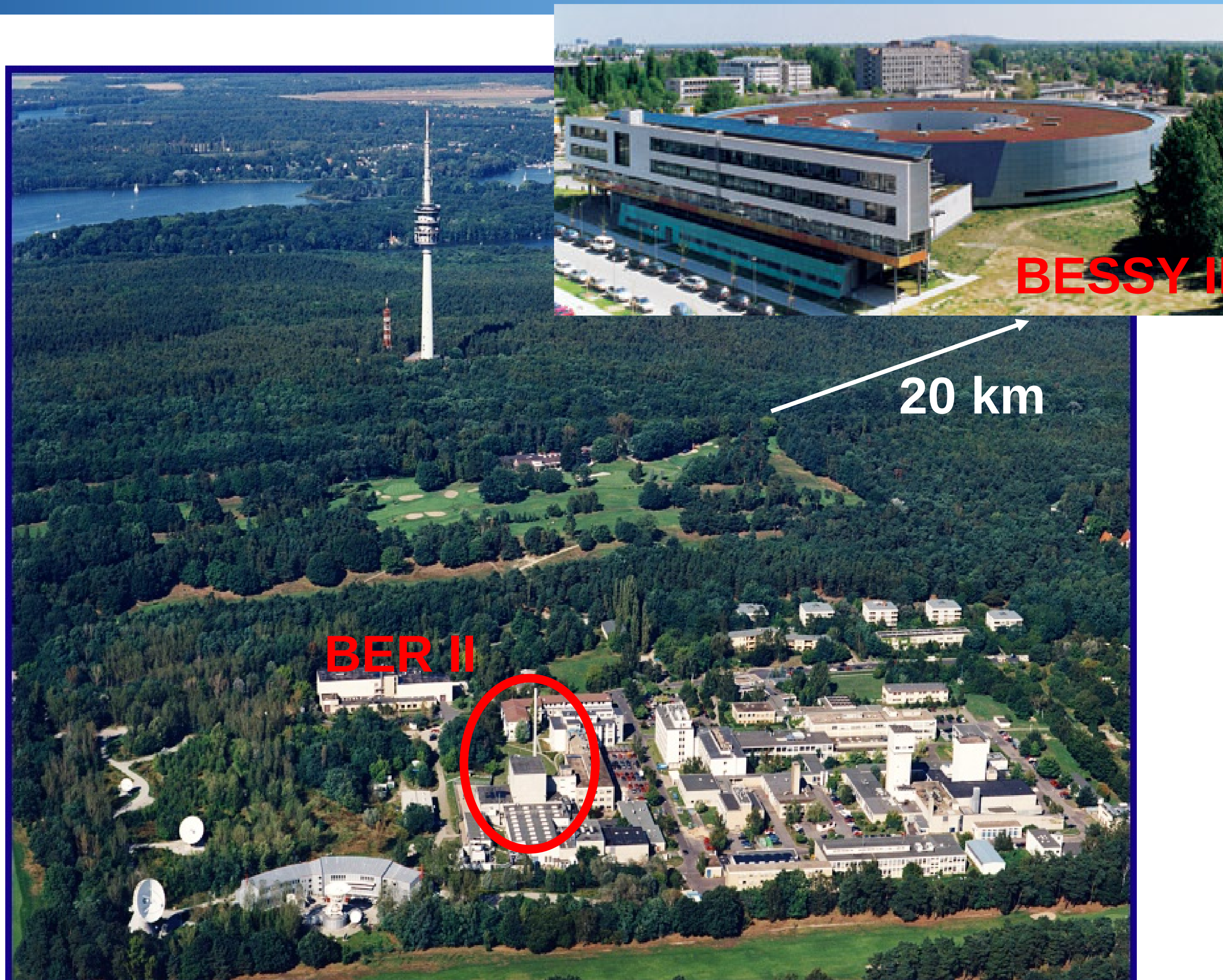

Introduction

Introduction

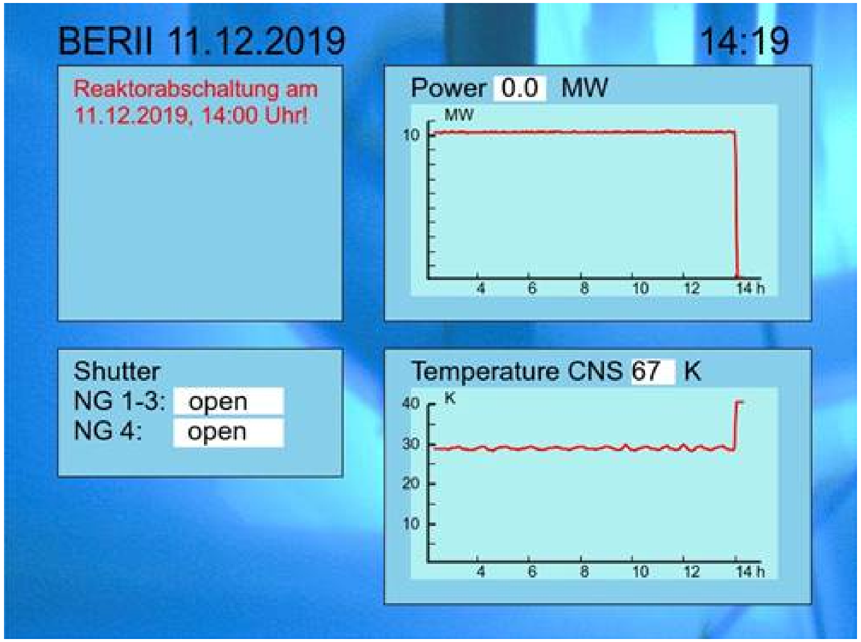

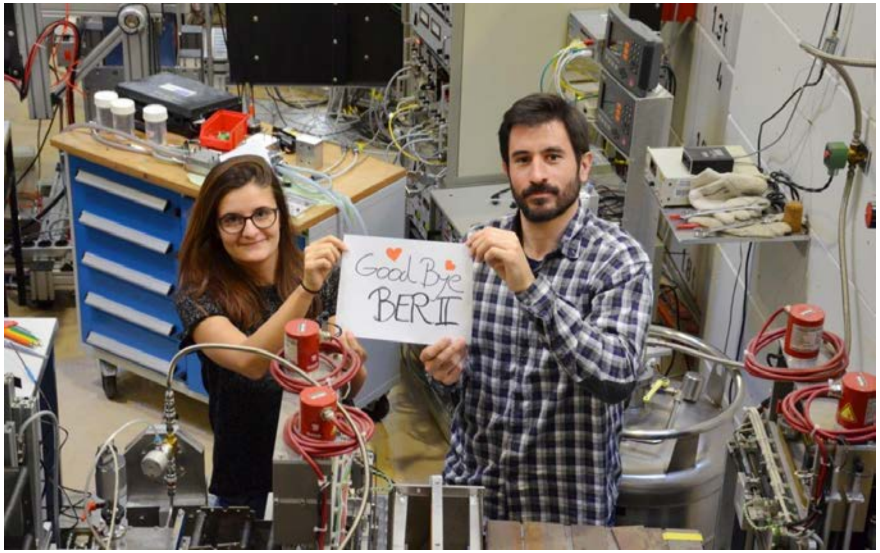

Joint Research Unit

HZB

Ni-Matters

since 2020

ILL UGA

Introduction

Institute of Applied Materials

Neutron ***Imaging*** *Micro CT* *Synchrotron*

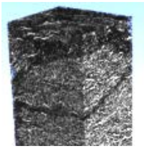

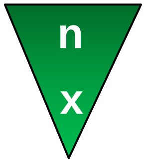

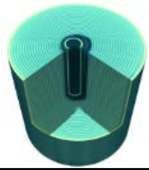

BAM-Line @ BESSY
Synchrotron tomography

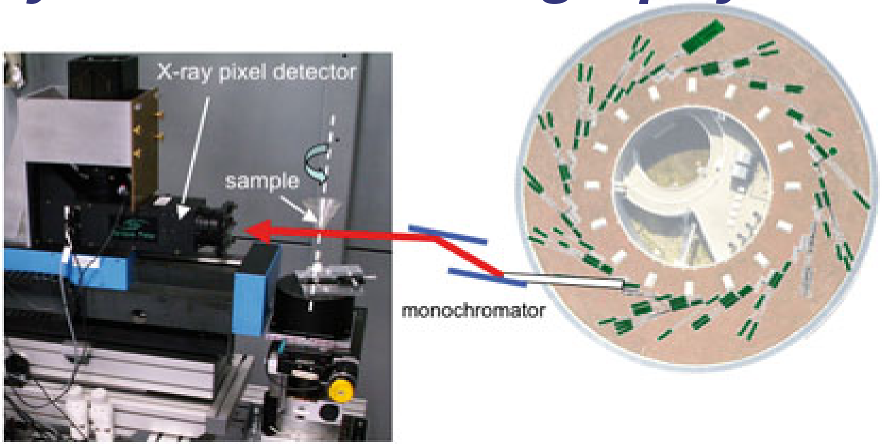

CONRAD-2 **2012 - 2019**
neutron tomography

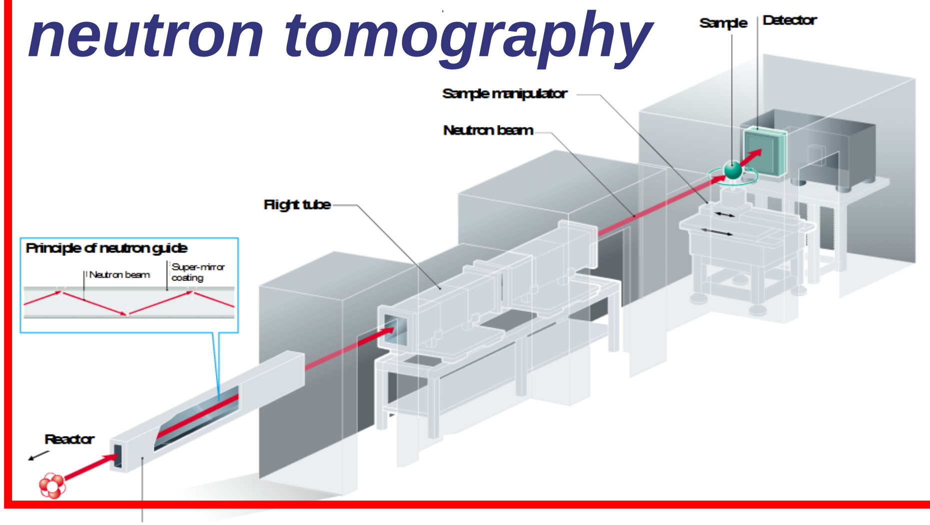

MicroCT Lab
X-ray tomography

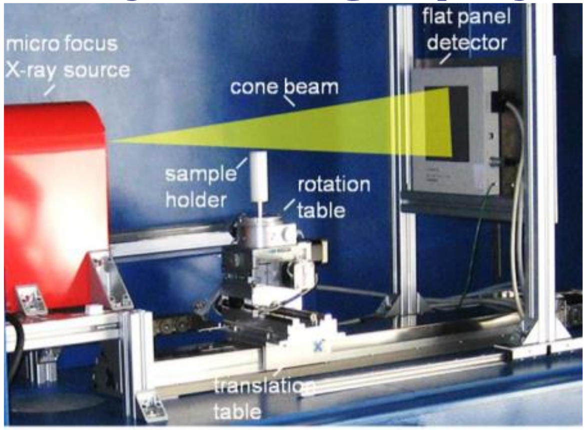

USER operation (2012-2019)

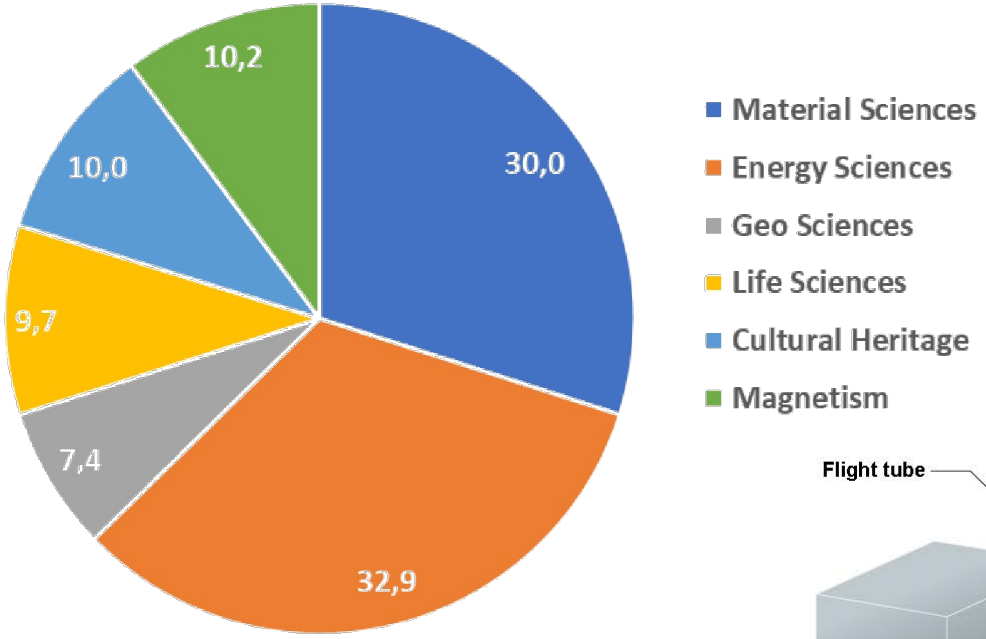

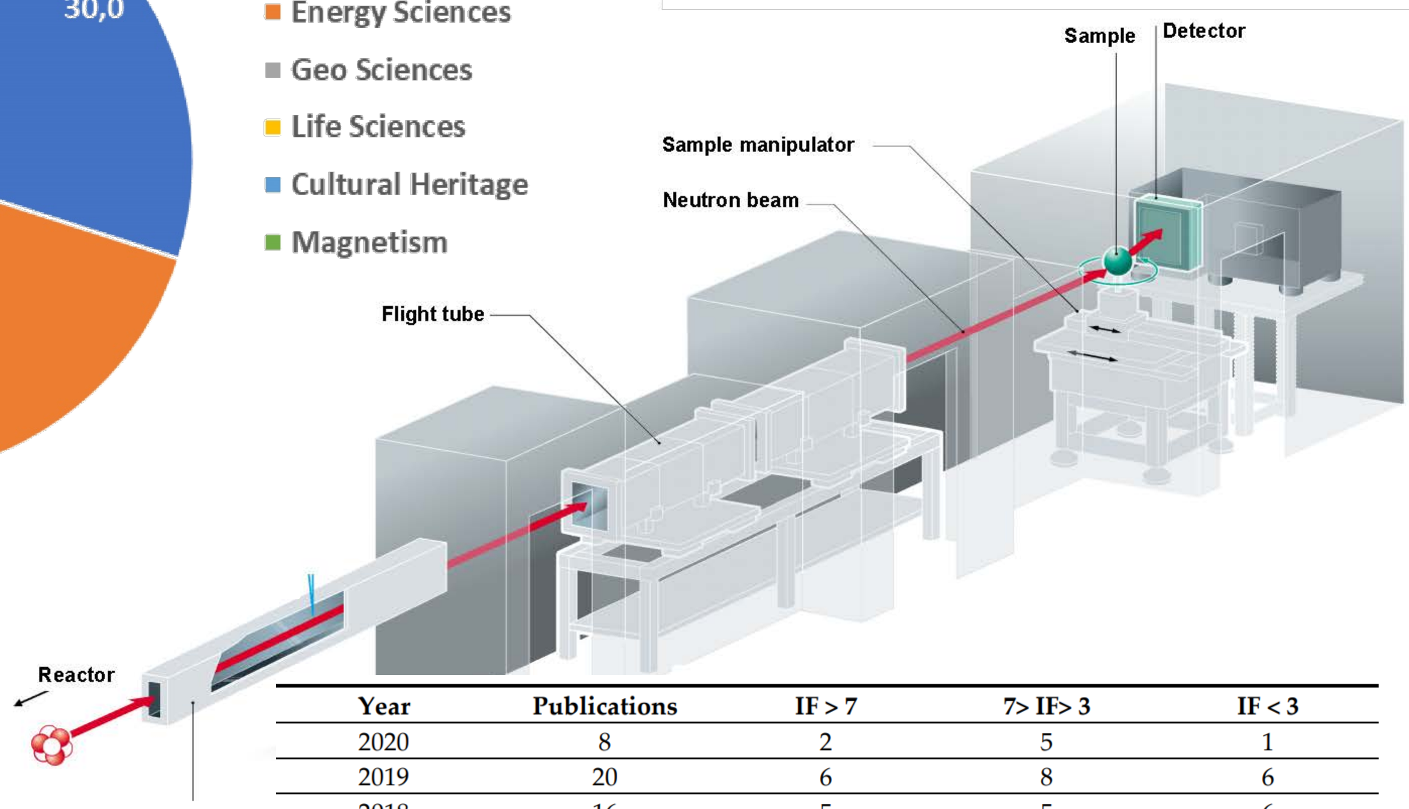

Year	Publications	IF > 7	7> IF> 3	IF < 3
2020	8	2	5	1
2019	20	6	8	6
2018	16	5	5	6
2017	16	2	6	8
2016	12	5	4	3
2015	25	3	4	18

HIGHLIGHTS FROM CONRAD-2 AND NEXT

4D imaging of lithium-batteries using correlative neutron and X-ray tomography with a virtual unrolling technique

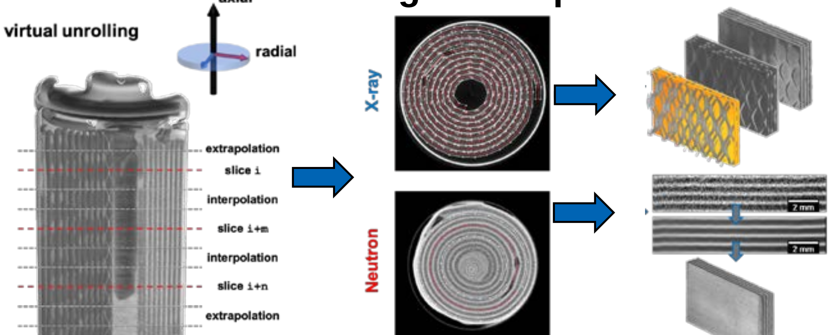

R.F. Ziesche (UCL, UK) *et al.*
Nature Communications 11, 1-11 (2020)

Tensorial neutron tomography of three-dimensional magnetic vector fields in bulk materials

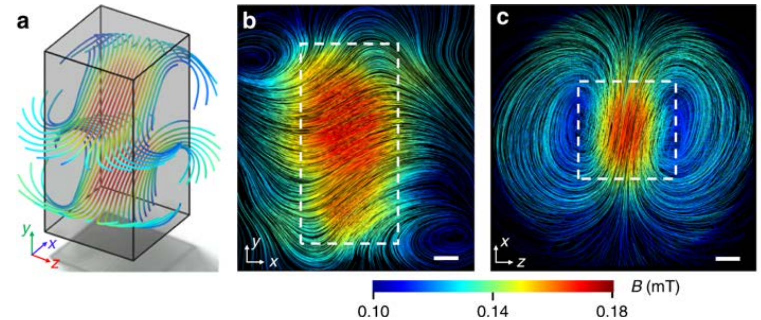

A. Hilger (HZB, EM-IAM) *et al.*
Nature Communications 9, 4023 (2018)

What comes NeXT?–High-speed neutron tomography at ILL

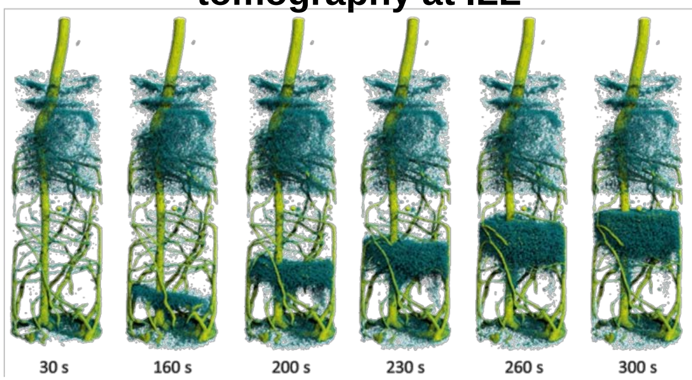

C. Tötzke (University of Potsdam) *et al.*
Optics express 27, 28640-28648, (2019)

Dynamic volume magnetic domain wall imaging in grain oriented electrical steel

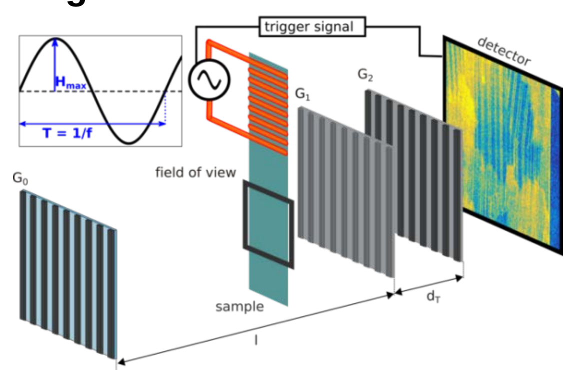

R. Harti (PSI, Switzerland) *et al.*
Scientific reports 8, 15754 (2018)

Adaptive high-resolution imaging
Dual-mode imaging (X+N)

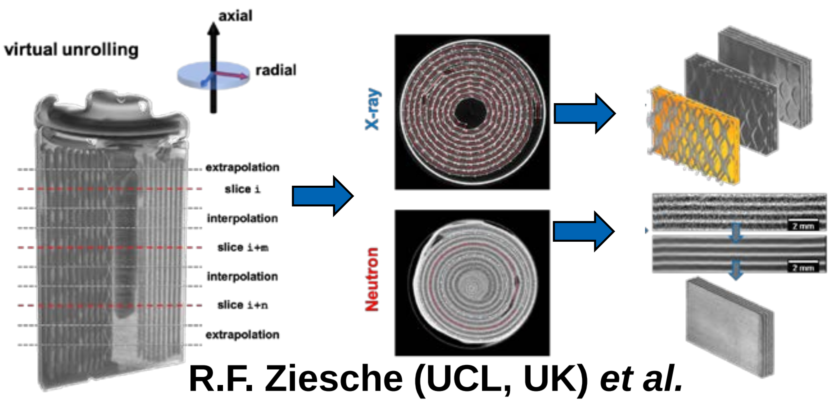

R.F. Ziesche (UCL, UK) *et al.*
Nature Communications 11, 1-11 (2020)

Tensorial magnetic tomography

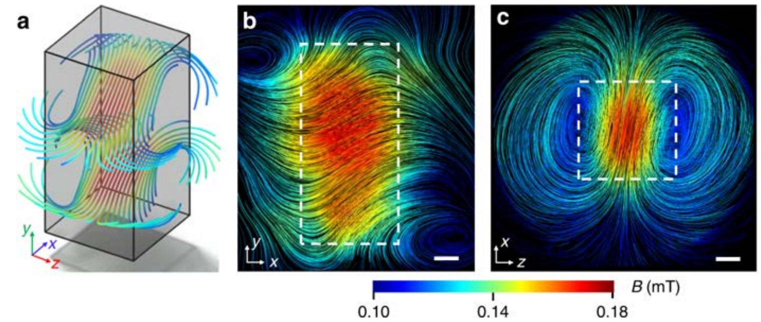

A. Hilger (HZB, EM-IAM) *et al.*
Nature Communications 9, 4023 (2018)

High-speed tomography of dynamic systems

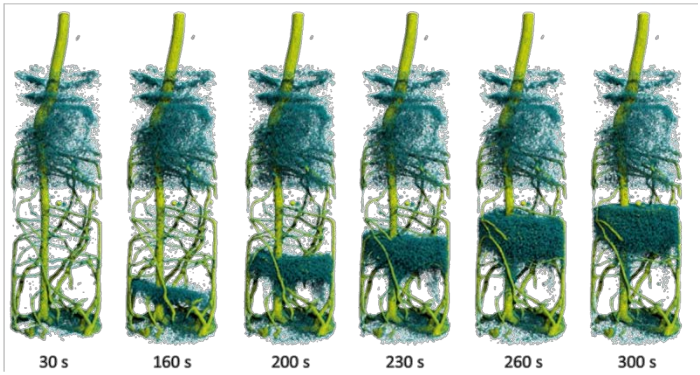

C. Tötzke (University of Potsdam) *et al.*
Optics express 27, 28640-28648, (2019)

Strobo-kinetic grating interferometry

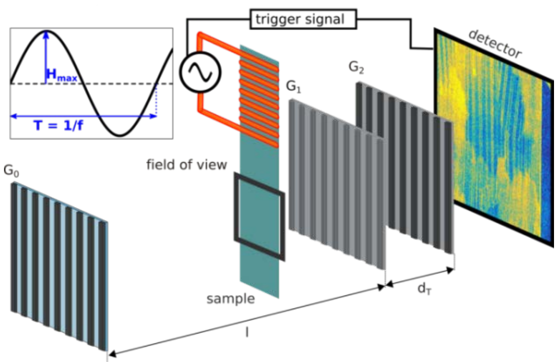

R. Harti (PSI, Switzerland) *et al.*
Scientific reports 8, 15754 (2018)

METHOD DEVELOPMENT HIGHLIGHTS

Adaptive **high-resolution** imaging
Dual-mode imaging (X+N)

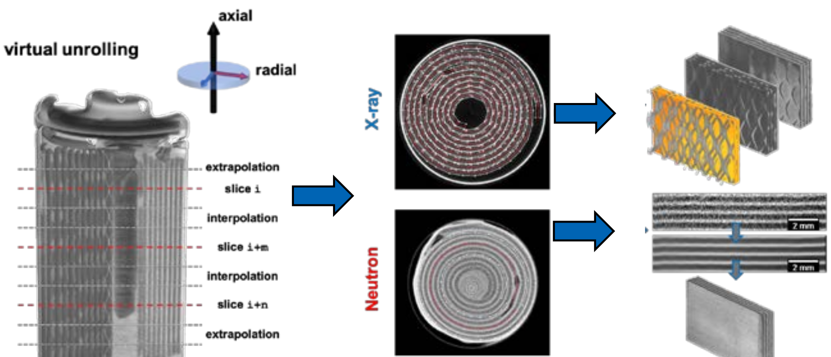

R.F. Ziesche (UCL, UK) *et al.*
Nature Communications 11, 1-11 (2020)

Tensorial magnetic tomography

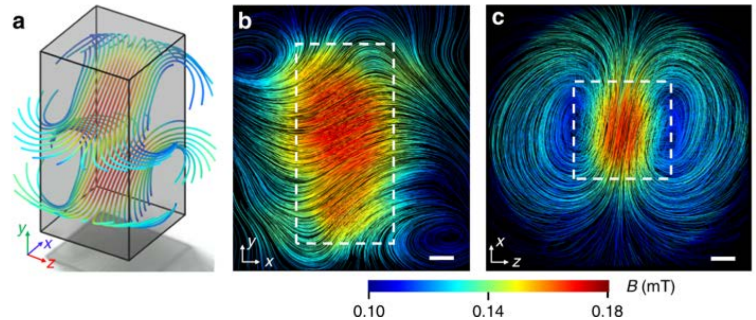

A. Hilger (HZB, EM-IAM) *et al.*
Nature Communications 9, 4023 (2018)

High-speed tomography of dynamic systems

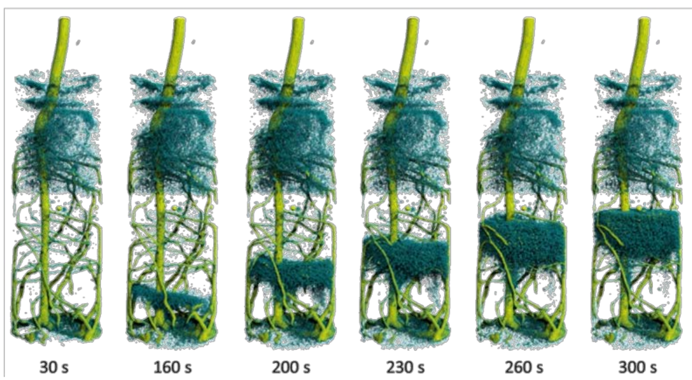

C. Tötzke (University of Potsdam) *et al.*
Optics express 27, 28640-28648, (2019)

Strobo-kinetic grating interferometry

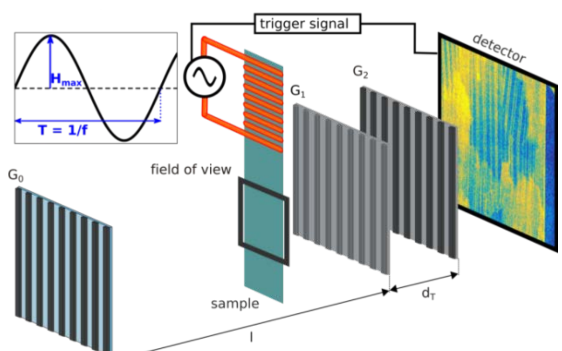

R. Harti (PSI, Switzerland) *et al.*
Scientific reports 8, 15754 (2018)

Motivation

The Olympic motto: **Citius, Altius, Fortius**

Faster, Higher, Stronger

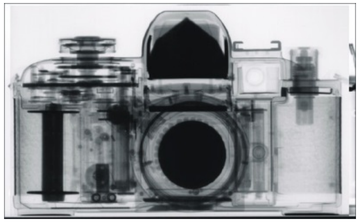

The Neutron Imaging motto:

Faster, Higher (Resolution), Larger

High spatial resolution

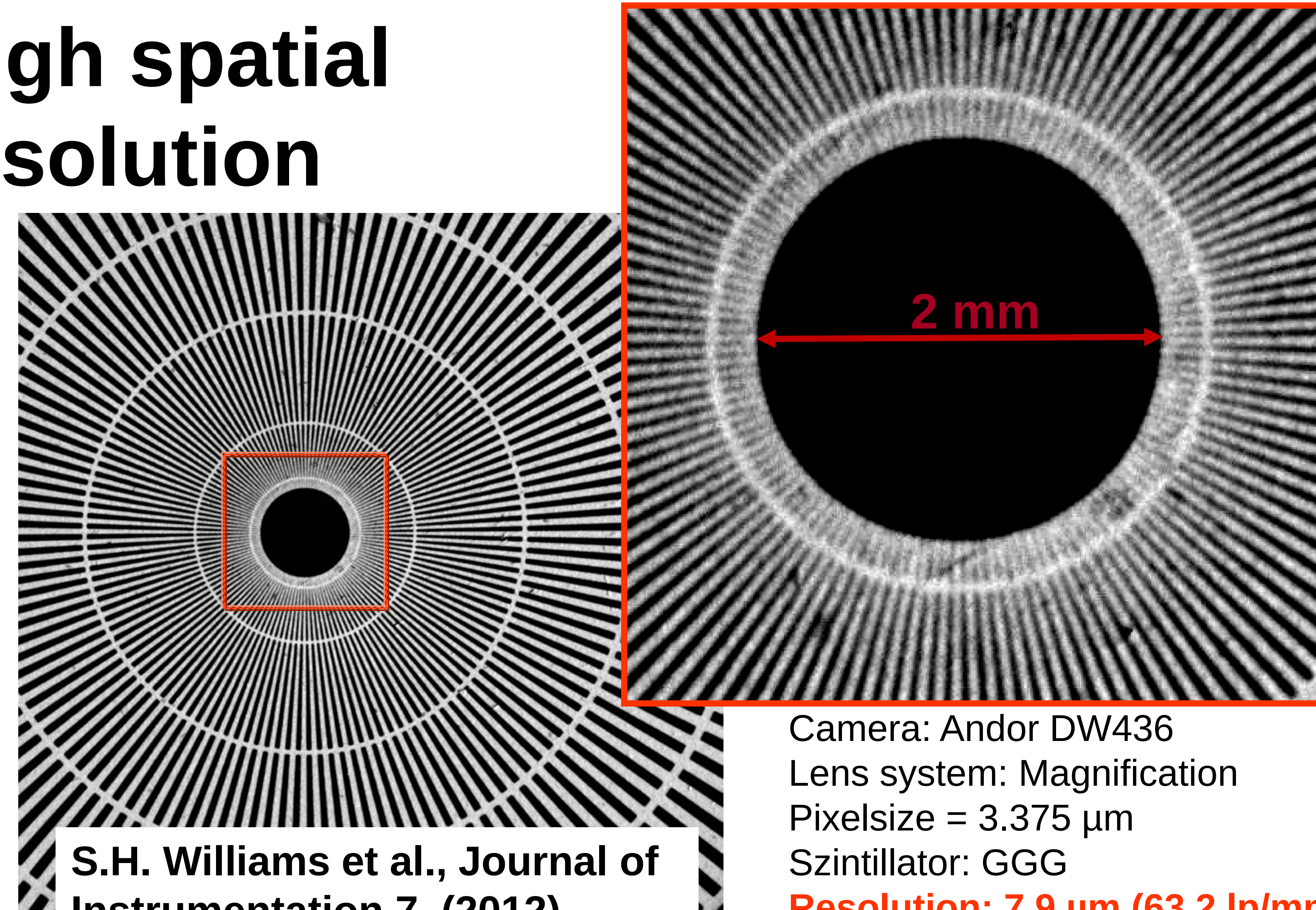

S.H. Williams et al., Journal of Instrumentation 7, (2012)

Camera: Andor DW436
Lens system: Magnification
Pixelsize = 3.375 µm
Szintillator: GGG
Resolution: 7.9 µm (63.2 lp/mm)

L/D ratio

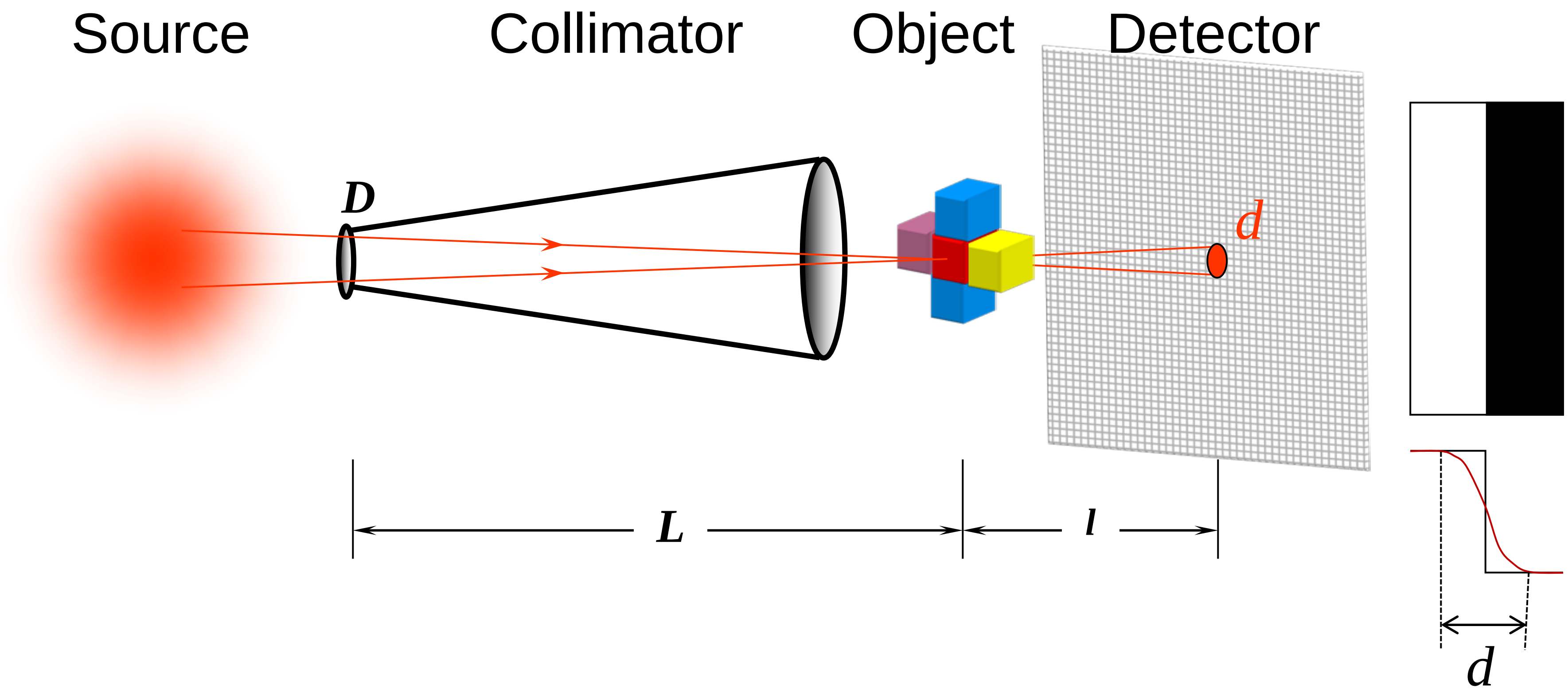

D – Collimator aperture

L – Distance Collimator-Object

l – Distance Object-Detector

$$d = \frac{l}{L/D}$$

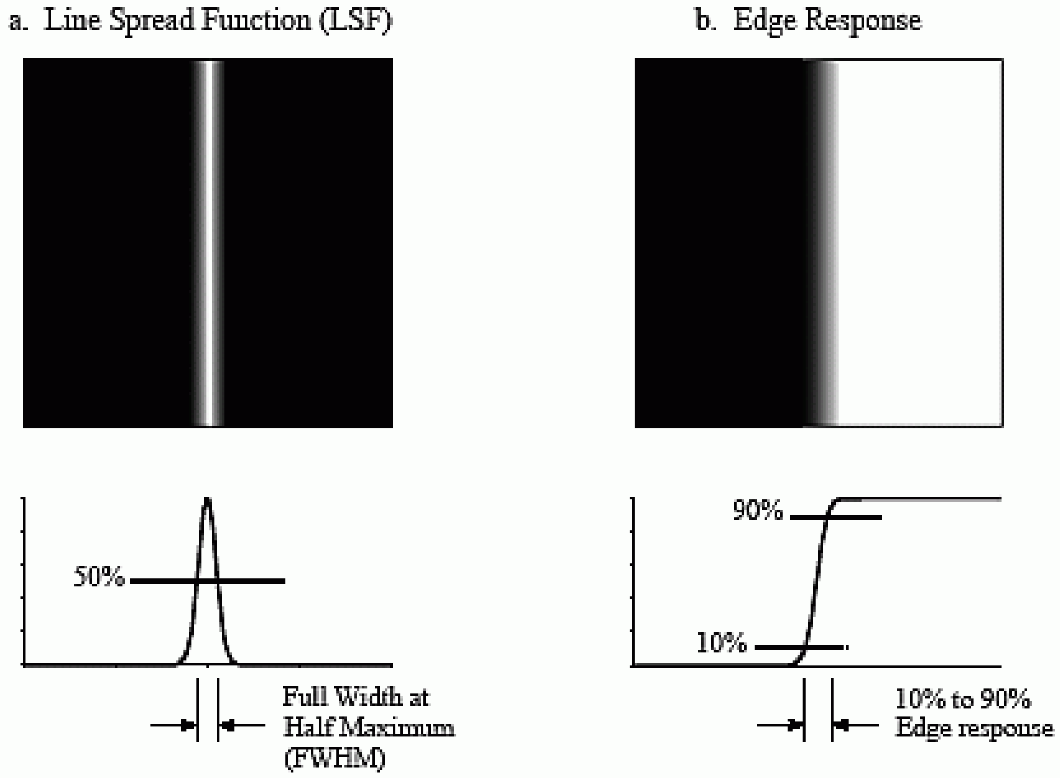

FIGURE 25-3
Line spread function and edge response. The line spread function (LSF) is the derivative of the edge response. The width of the LSF is usually expressed as the Full-Width-at-Half-Maximum (FWHM). The width of the edge response is usually quoted by the 10% to 90% distance.

Detector characterization

Spatial resolution

MTF is the *spatial* frequency response of an imaging system or a component; it is the contrast at a given spatial frequency relative to low frequencies.

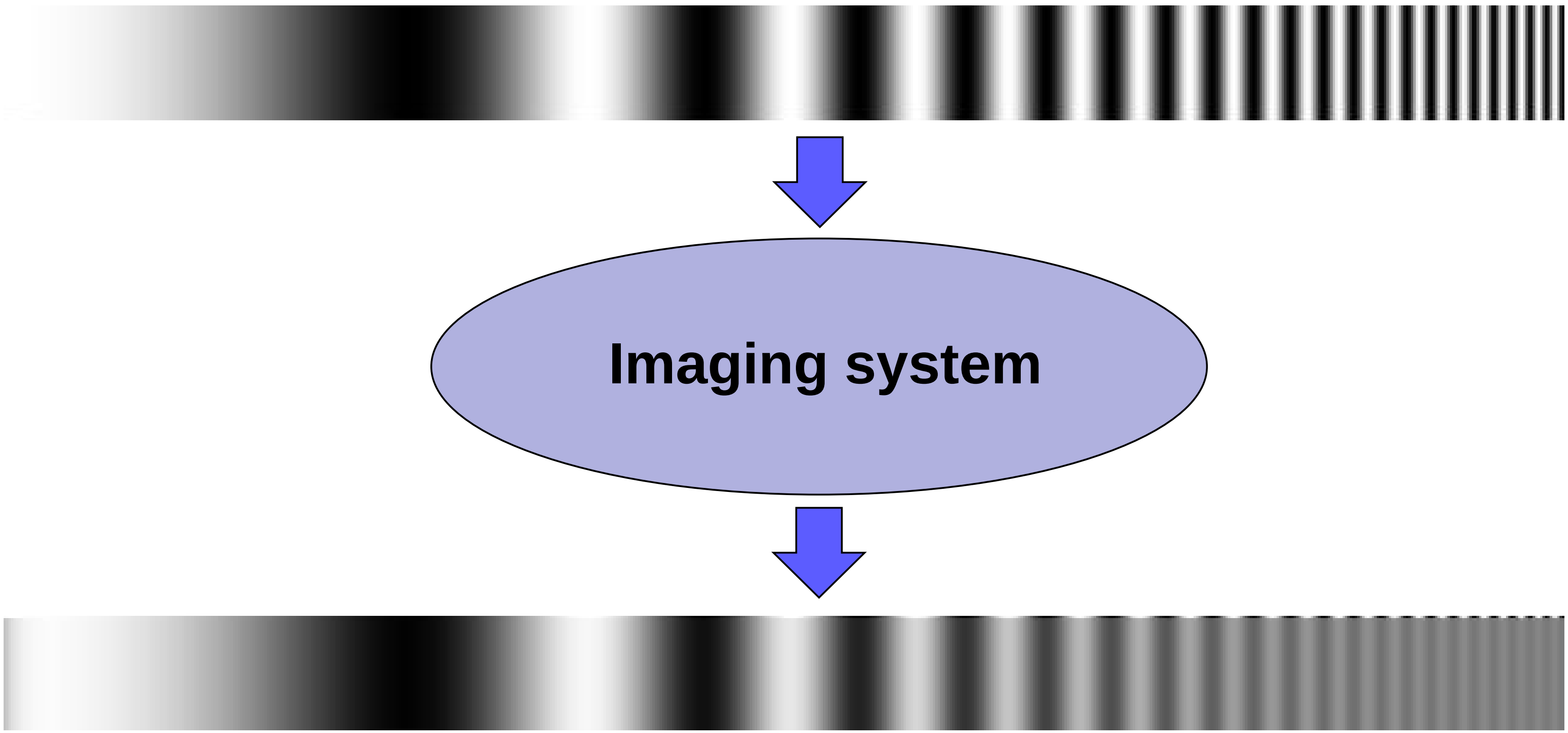

http://www.normankoren.com/Tutorials/MTF.html

Spatial resolution & contrast

Contrast levels

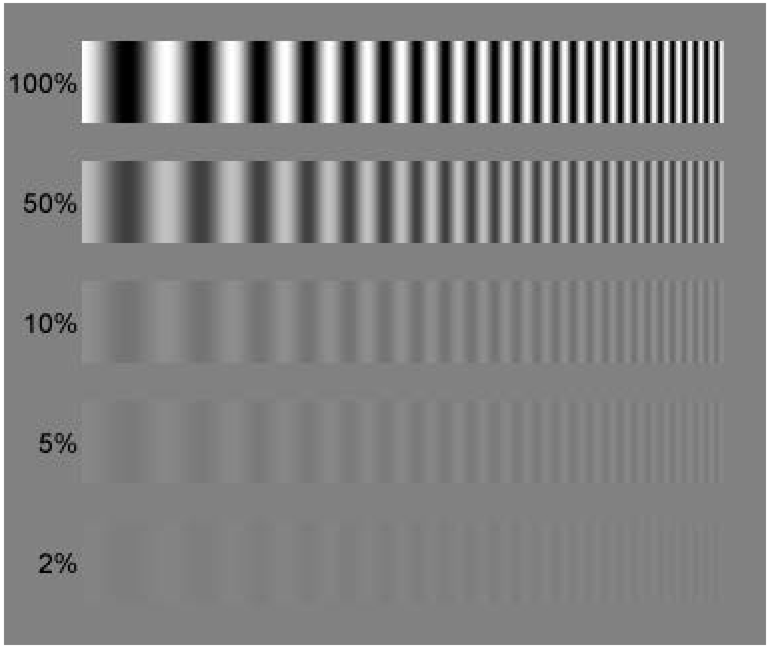

Frequence response: MTF

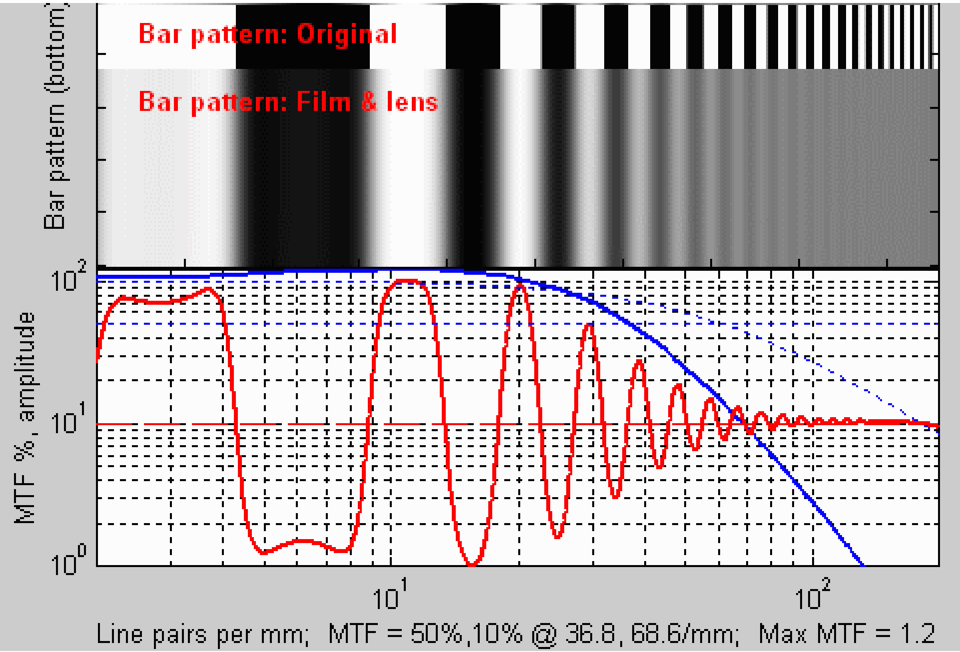

http://www.normankoren.com/Tutorials/MTF.html

Spatial resolution

Scintillator: 5 µm Gadox
Lens system: 200 mm
Pixel size: 15 µm
Exposure time: 150 s

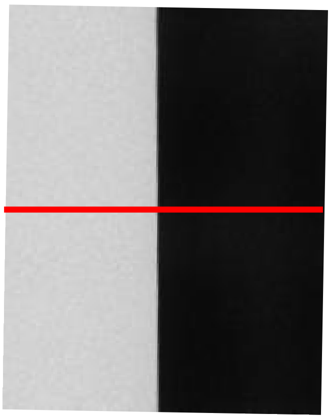

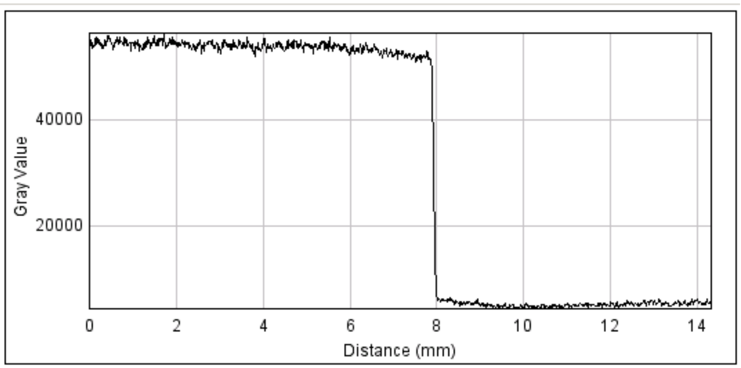

20 lp/mm ~ 25 µm

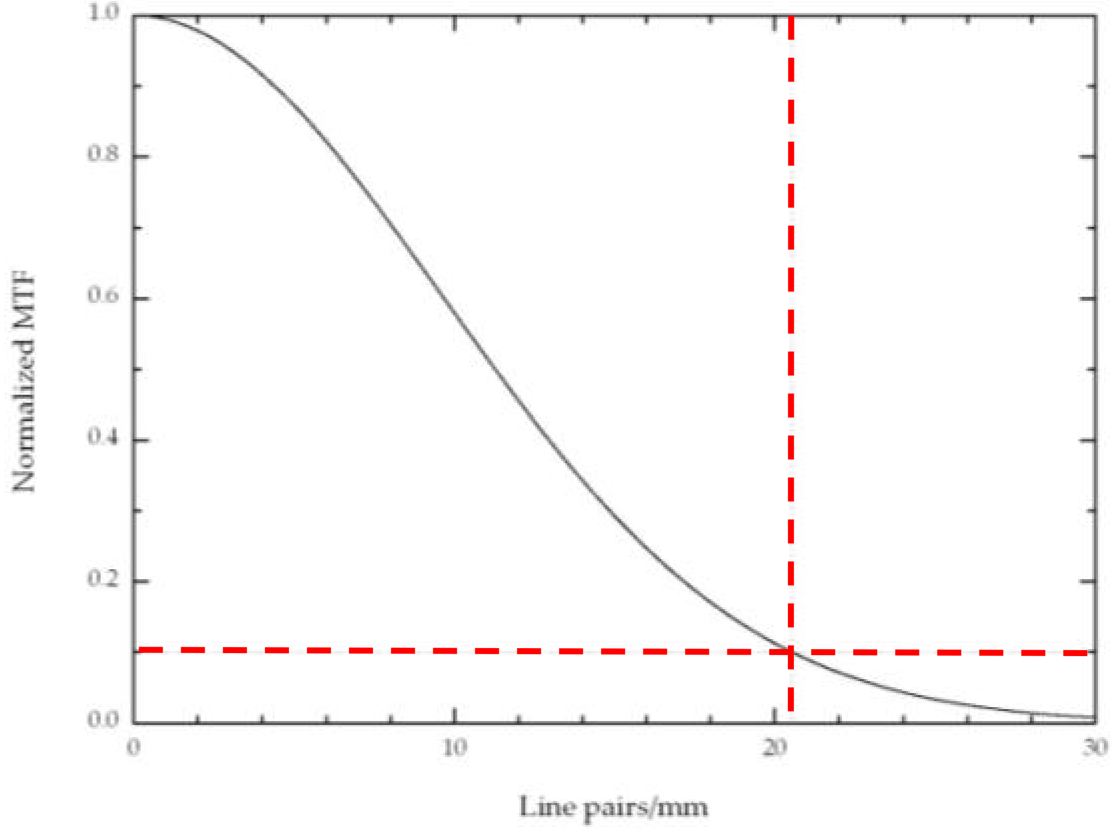

N. Kardjilov, et al. "A highly adaptive detector system for high resolution neutron imaging." *Nuclear Instruments and Methods in Physics Research Section A* 651.1 (2011): 95-99.

High resolution NI

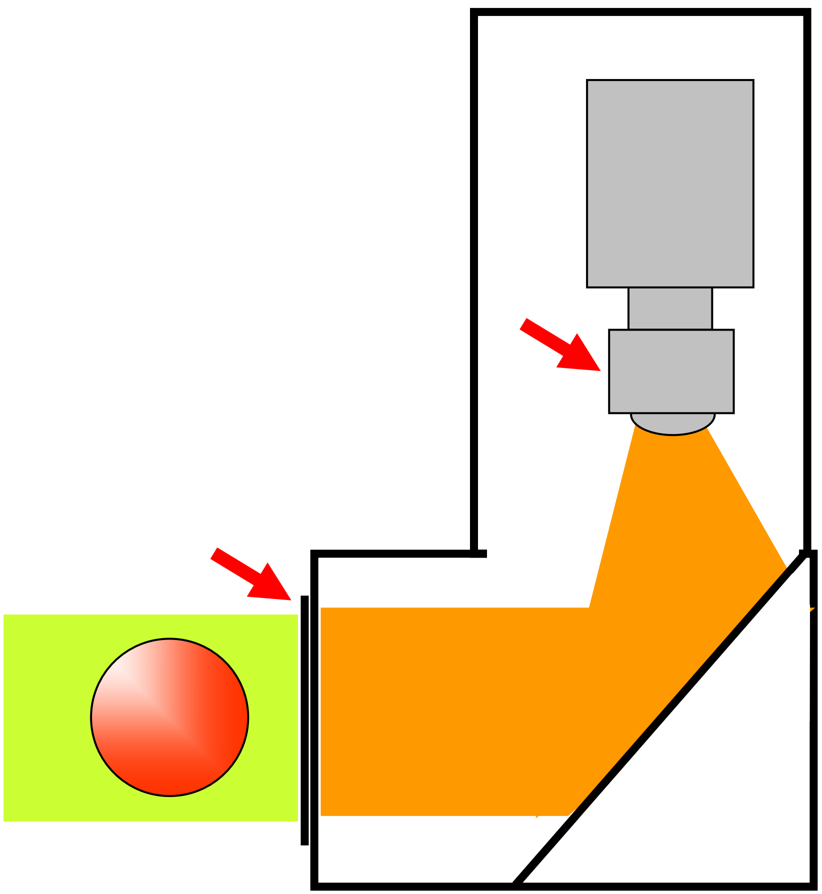

Standard setup (2006)

Scintillator: 200 µm 6LiF
Lens system: 50 mm
Pixel size: 100 µm
Exposure time: 20 s

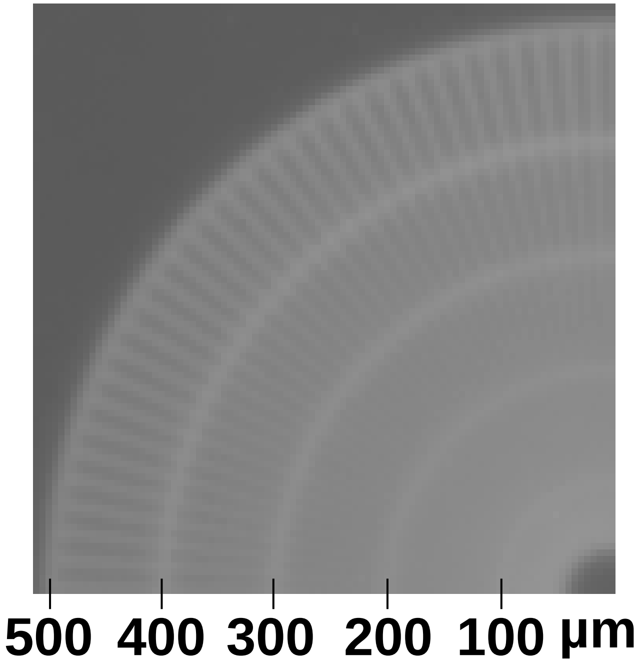

Detector system

CCD camera:
ANDOR DW-436

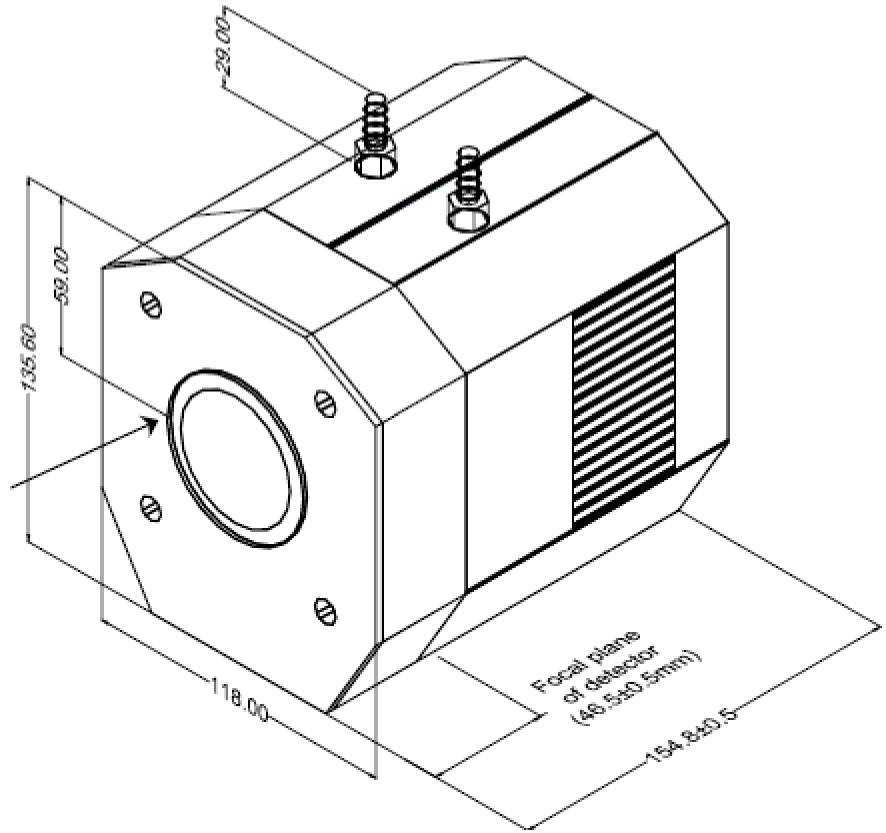

●Sensor	Active Pixels	2048 x 2048	Dummy Pixels *1	50, 50, 0, 0
	Pixel Size (μm²)	13.5	Image Area (mm)	27.6 x 27.6
	Pixel Well Depth (e⁻, typical)	80,000	Register Well Depth (e⁻, typical) *2	600,000
	Linearity (%, maximum) *3	1	Gain (e⁻/count @ 1&2, 16, 32 μs)	2, 1.4, 0.7
	Vertical Clock Speed (μs)	112		

Lens systems

Nikkor Makro-Objektiv - 105 mm - F/2.8

FOV_{max}: 10 cm x 10 cm, pixel size: 50 µm
FOV_{min} : 6 cm x 6 cm, pixel size: 30 µm

Nikon Micro Nikkor 200mm f/4 D (IF) ED

1:1 imaging
FOV_{max}: 2.8 cm x 2.8 cm, pixel size: 13.5 µm

N. Kardjilov, et al. "A highly adaptive detector system for high resolution neutron imaging." *Nuclear Instruments and Methods in Physics Research Section A* 651.1 (2011): 95-99.

Scintillators

neutron detection for imaging

- no direct neutron detection possible
- a secondary nuclear process is needed
  (capture, fission, collision)
- main ***neutron imaging processes*** are using:
  - scintillation
  - photo-luminiscence by secondary particles + β, γ
  - nuclear track detection
  - chemical excitation
  - collection of charge in semiconductors from Gd conversion

Capture reactions for thermal / cold neutrons

$^{3}He + {}^{1}n \Rightarrow {}^{3}He + {}^{1}p + 0.77\ MeV$

→ $^{6}Li + {}^{1}n \Rightarrow {}^{3}H + {}^{4}He + 4.79\ MeV$

$^{10}B + {}^{1}n \Rightarrow {}^{7}Li + {}^{4}He + 2.78\ MeV$ (7%)

$\Rightarrow {}^{7}Li^{*} + {}^{4}He + 2.30\ MeV$ (93%)

$^{155}Gd + {}^{1}n \Rightarrow {}^{156}Gd + \gamma$´s + CE´s (7.9 MeV)

→

$^{157}Gd + {}^{1}n \Rightarrow {}^{158}Gd + \gamma$´s + CE´s (8.5 MeV)

^{235}U, ^{239}Pu $^{1}n \Rightarrow$ fission products + 80 MeV

The ZnS+^{6}LiF scintillation screen is the limit of resolution.

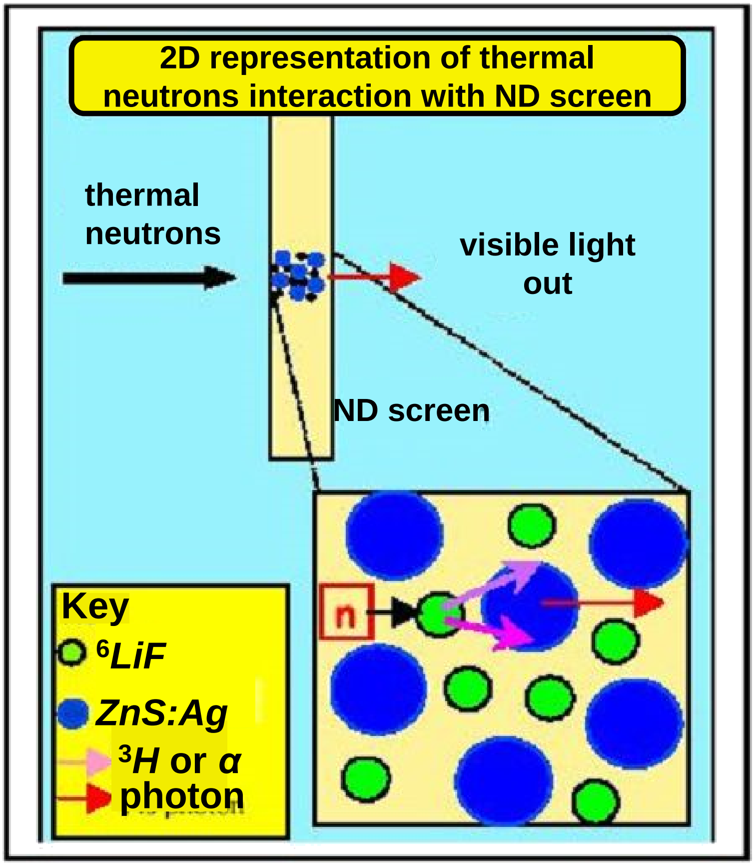

The reaction products of

^{6}Li(n,α) ->^{3}H + ^{4}He + 4.7 MeV

have to be stopped in the ZnS scintillation screen.
Their average range is in the order of 50-80 μm.

About 177,000 photons are generated per detected neutron.

With thinned scintillation screens, we can achieve resolution in the order of 20-30 μm.

Slide courtesy: Dr. Burkhard Schillinger (FRM-II, Munich, Germany)

Scintillators, effect of thickness

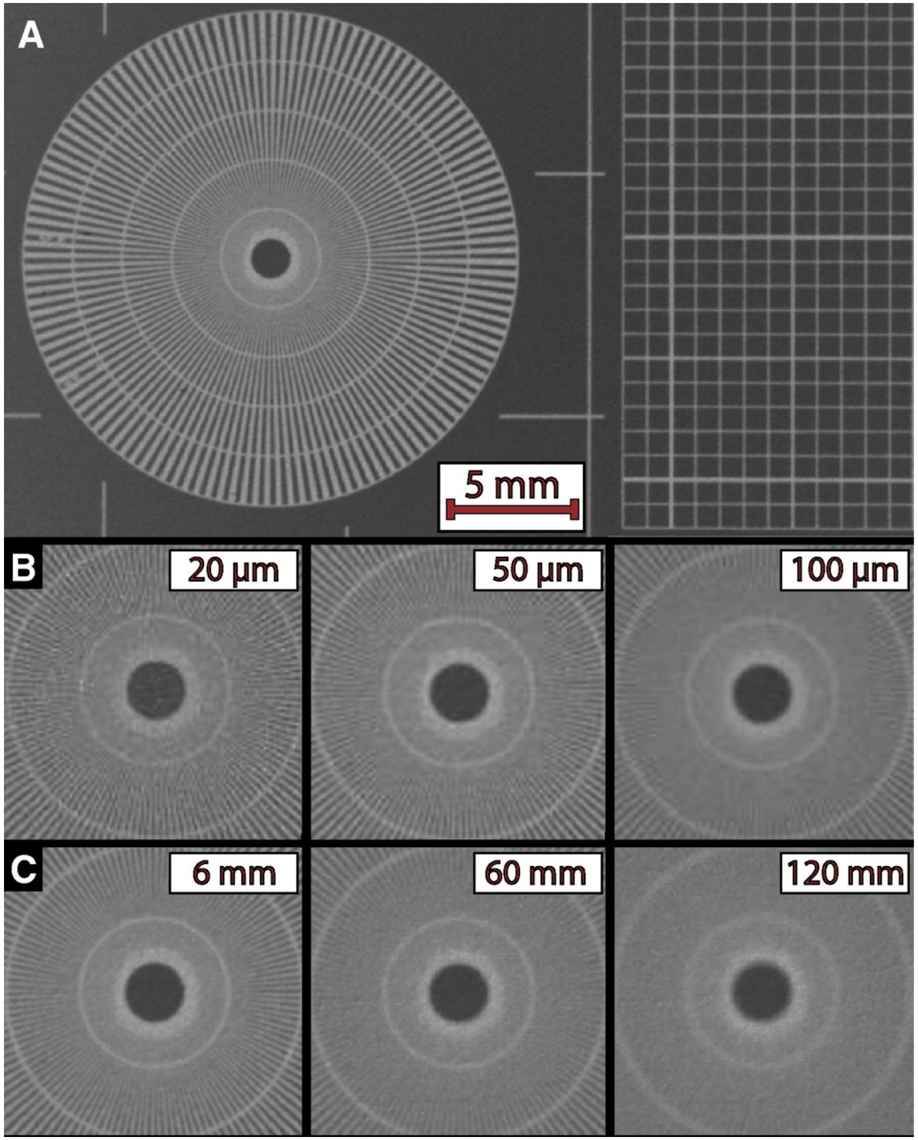

(A) A radiograph of the Siemens star test pattern used to study the effect of scintillator thickness, exposure time, and impact of geometrical blurring.
(B) Images showing the center of the Siemens star for scintillators of different thicknesses.
(C) The same region imaged by a scintillator of 50 µm thickness. In each image the test pattern is placed further away from the scintillator, resulting in increased geometrical blurring.

K.-U. Hess et al., Advances in high-resolution neutron computed tomography: Adapted to the earth sciences , Geosphere (2011) 7 (6): 1294-1302.

Standard setup

Scintillator: 200 µm 6LiF
Lens system: 50 mm
Pixel size: 100 µm
Exposure time: 20 s

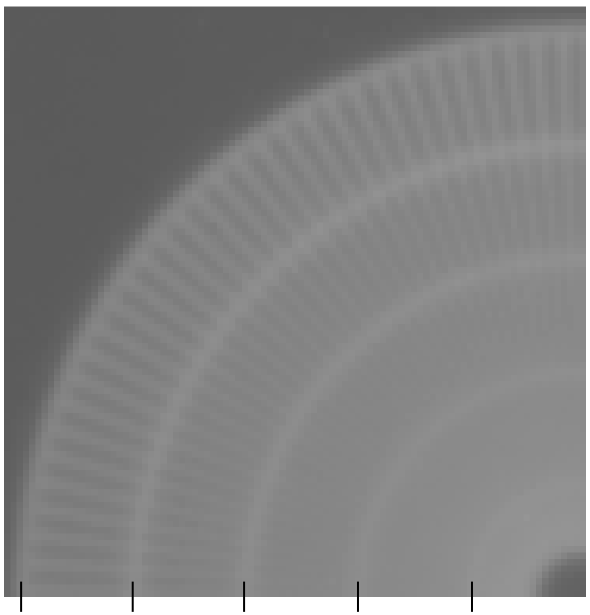

Improved lenses

Scintillator: 200 µm 6LiF
Lens system: 105 mm
Pixel size: 30 µm
Exposure time: 20 s

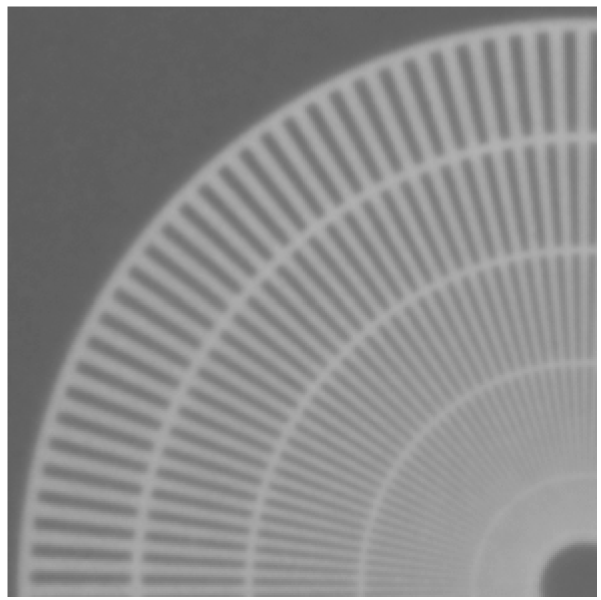

+ Improved screen

Scintillator: 5 µm Gadox
Lens system: 105 mm
Pixel size: 30 µm
Exposure time: 120 s

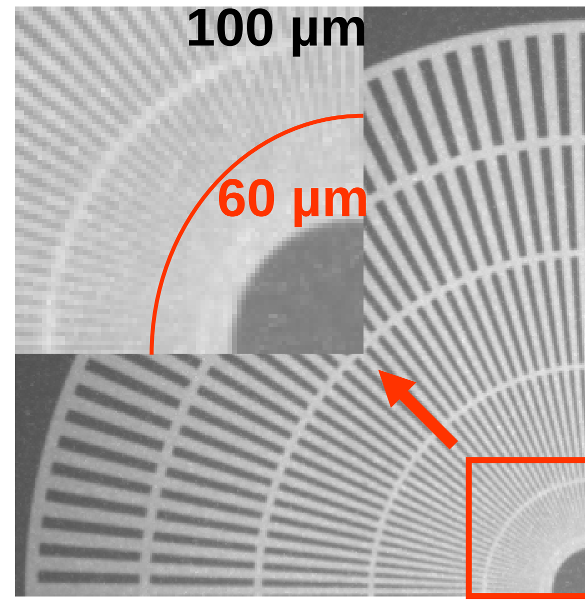

N. Kardjilov, et al. "A highly adaptive detector system for high resolution neutron imaging." *Nuclear Instruments and Methods in Physics Research Section A* 651.1 (2011): 95-99.

High resolution

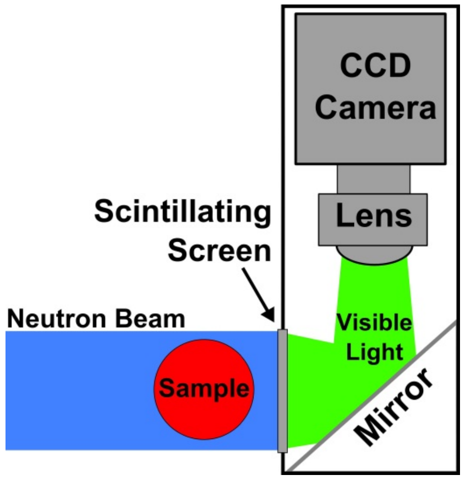

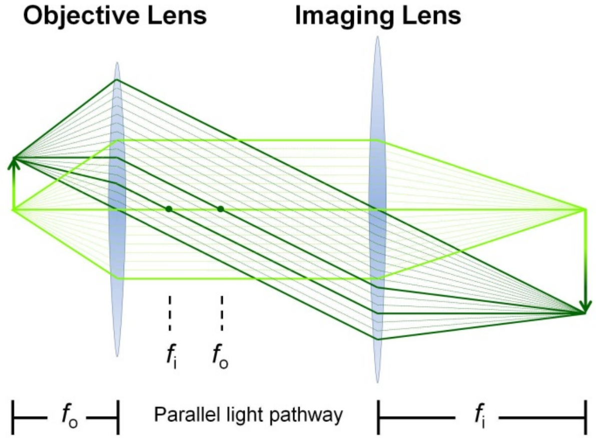

10 µm Gadox

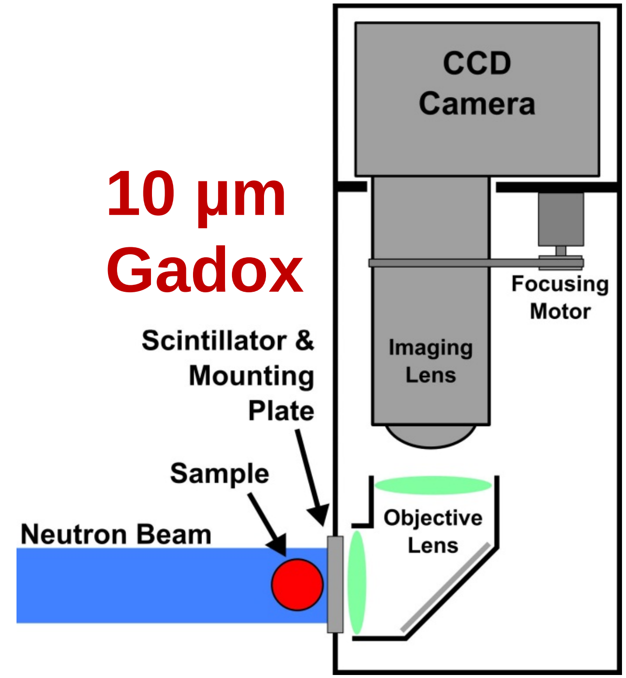

Obj. Lens/Img. Lens	*M*	$P_{\rm eff}$ *(µm)*	*FOV (mm)*
105 mm / 50 mm	2.10	6.429	13.2 × 13.2
200 mm / 100 mm	2.00	6.750	13.8 × 13.8
200 mm / 50 mm	4.00	3.375	6.9 × 6.9

S. H. Williams et al, J. of Instrumentation (2012)

Attenuation Contrast

Fuel cells

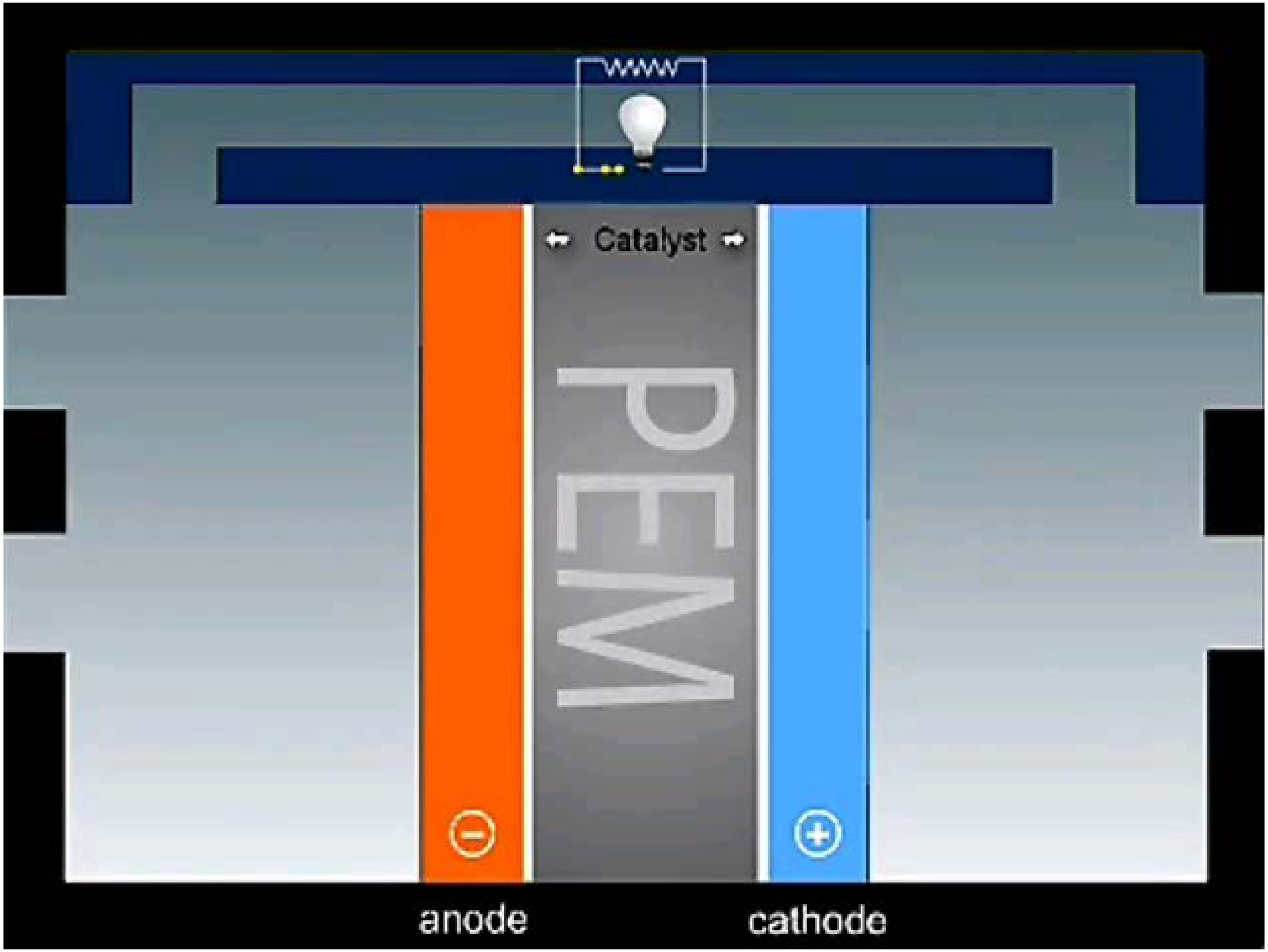

Attenuation Contrast

Fuel cells

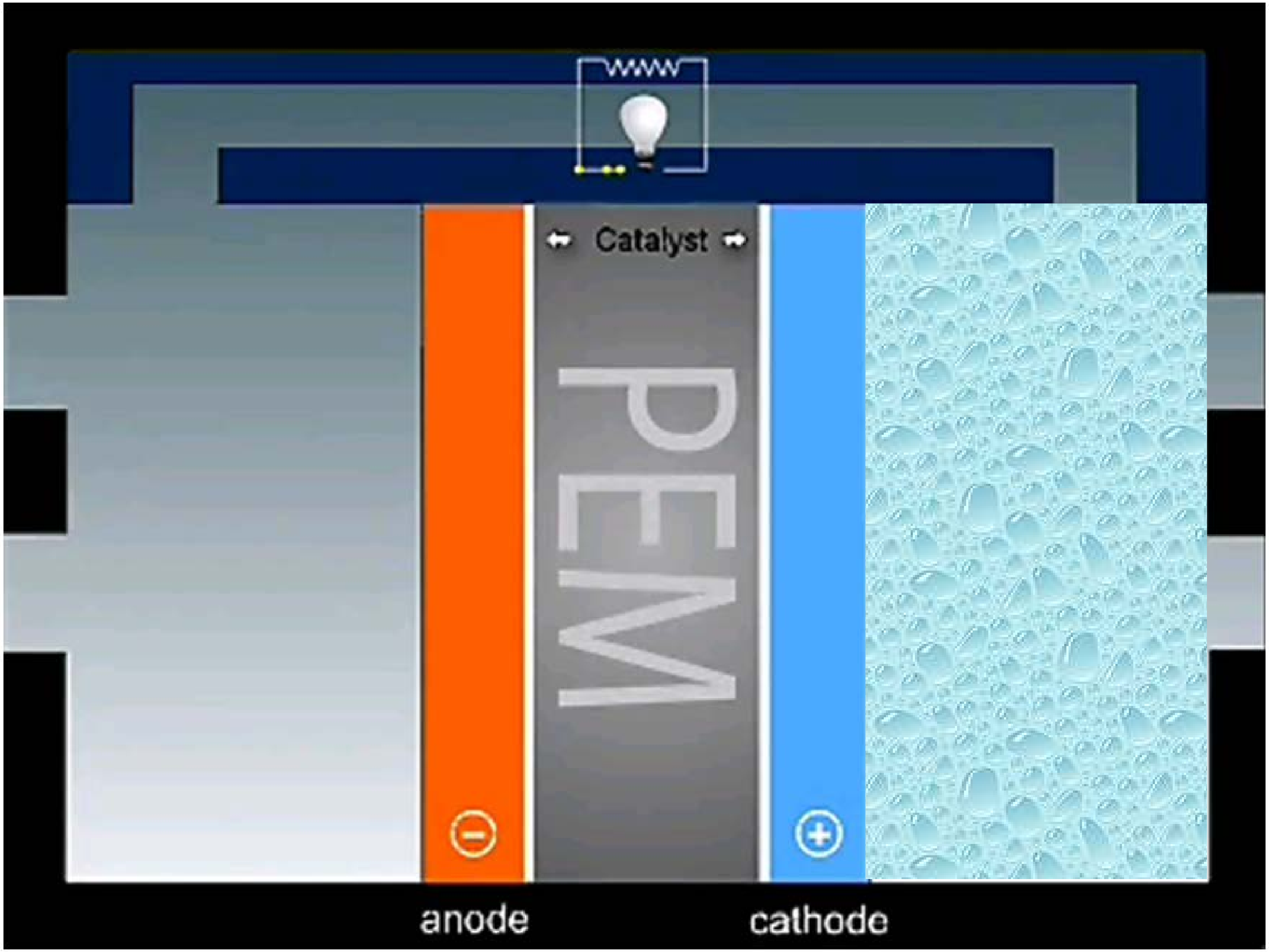

Alexander Bauder

Robert Alink

Jan Haußmann
Joachim Scholta

J. Haußmann *et al.*,
Journal of Power Sources 239 (2013) 611

How to optimize water management in a PEM fuel cell?

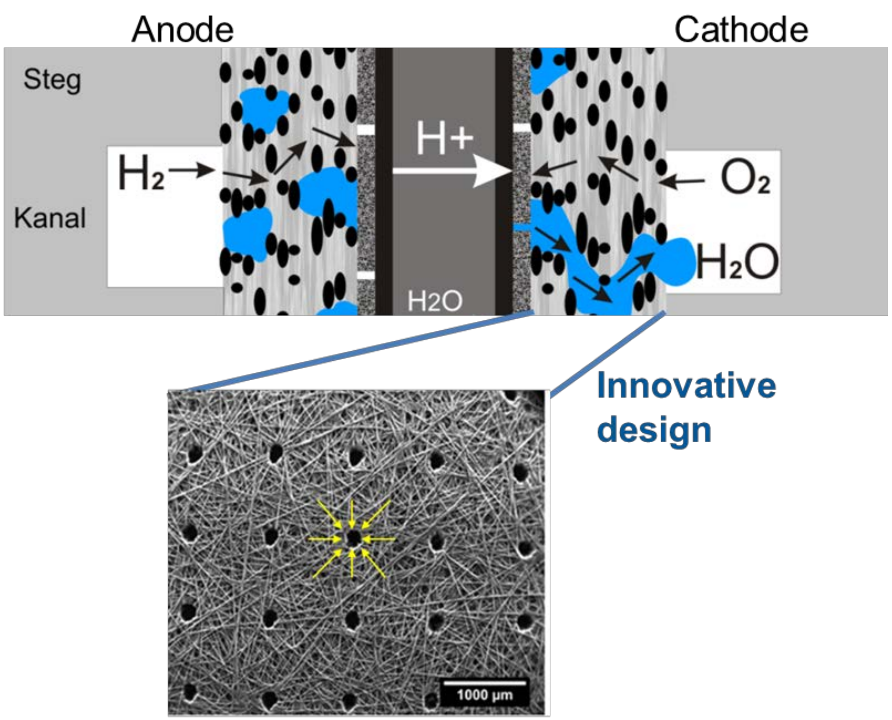

Perforation = Drainage effect

- ***In-operando*** **visualization of water distribution**

Diffusion dynamics revealed with D-H contrast

Photons: tailor-made microporosity improves water transport

→ Optimized electrode design

➡ Improved performance under varying operation conditions

Alexander Bauder
Robert Alink
Jan Haußmann
Joachim Scholta

J. Haußmann *et al.*,
Journal of Power Sources 239 (2013) 611

How to optimize water management in a PEM fuel cell?

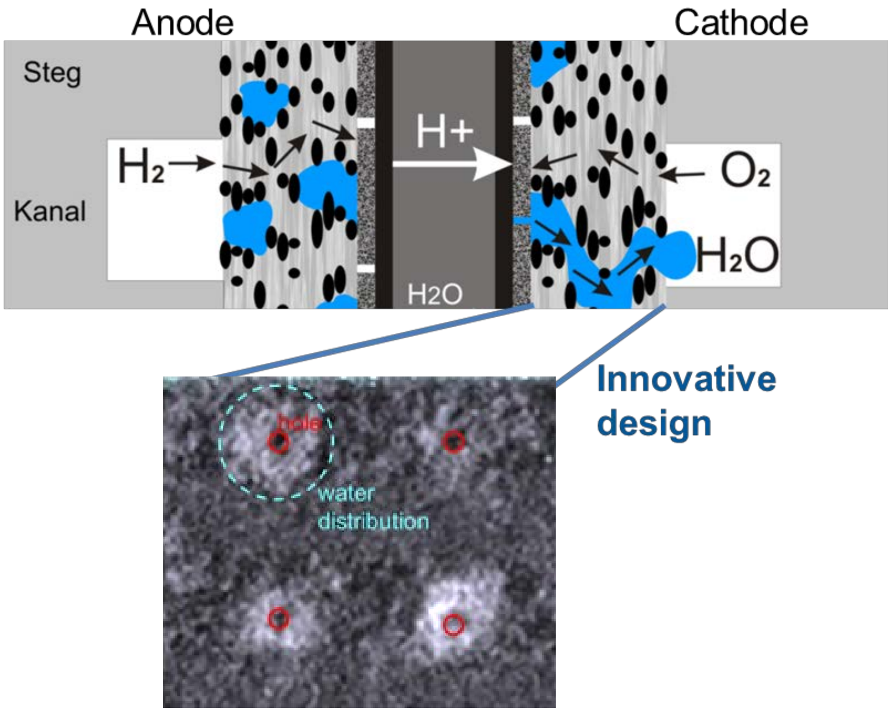

Neutron tomography slice
(pixel size: 6.5 µm, 600 projections /360°, time: 8 h)

- ***In-operando* visualization of water distribution**

Diffusion dynamics revealed with D-H contrast

Photons: tailor-made microporosity improves water transport

➔ **Optimized electrode design**

➡ **Improved performance under varying operation conditions**

Attenuation Contrast

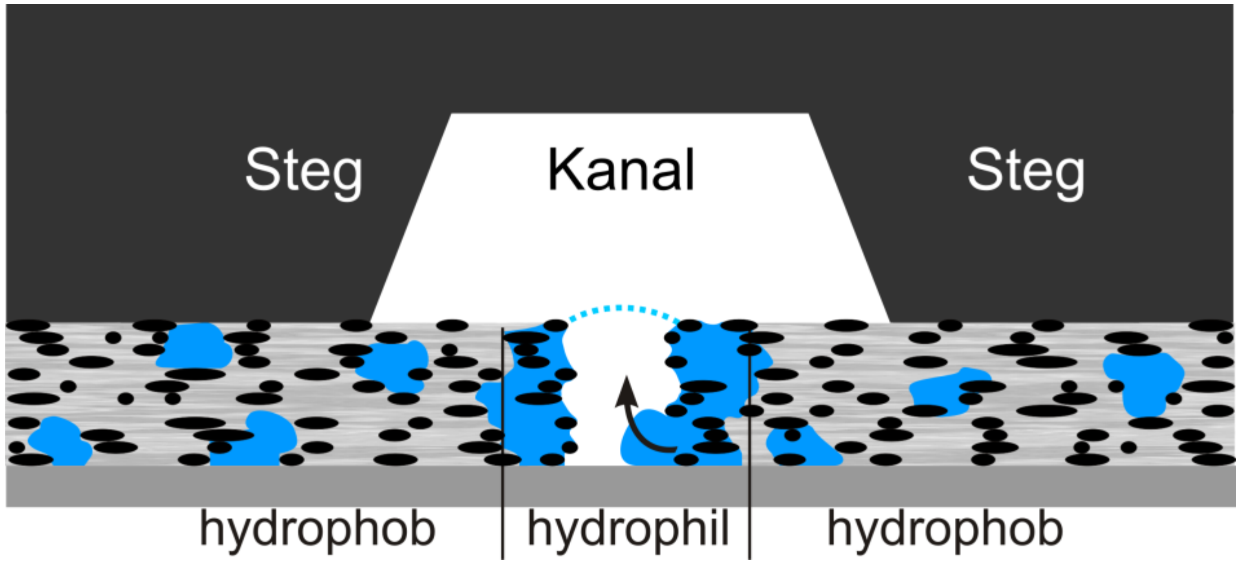

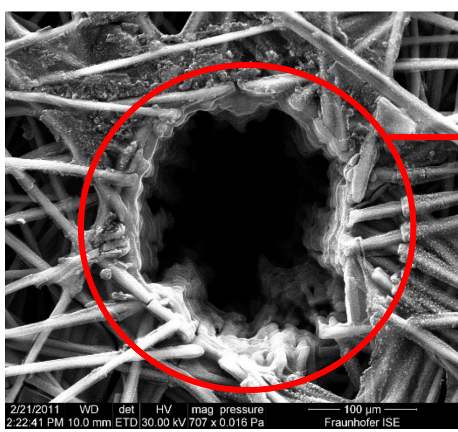

Heat affected zone

Hydrophilic areas cause water agglomerations

Fuel Cell Research

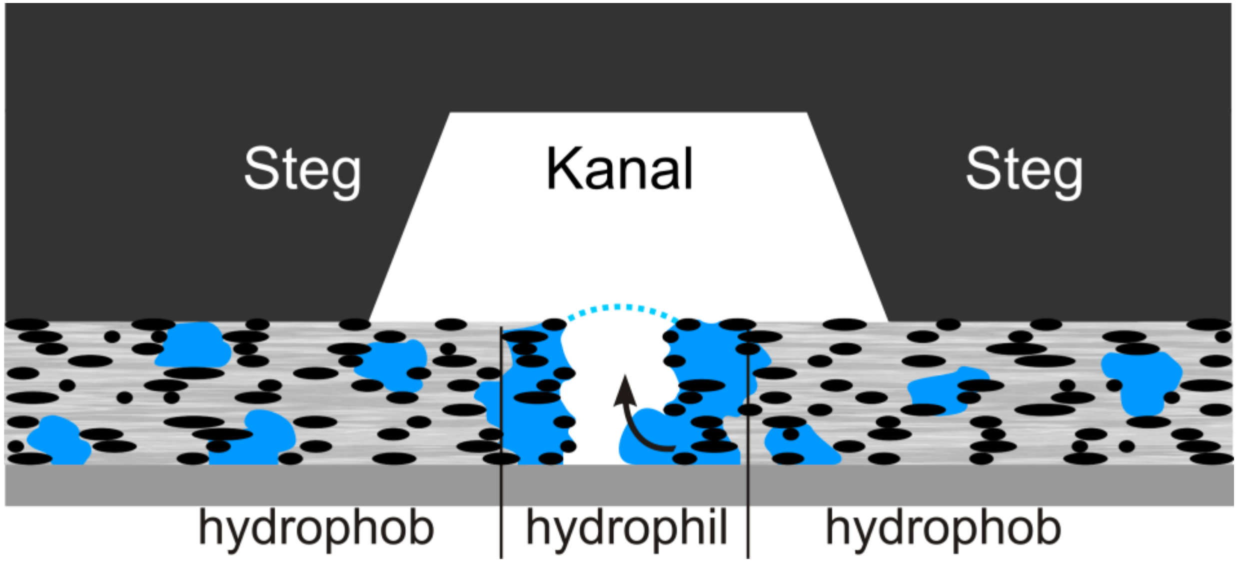

BESSY II

laser perforation

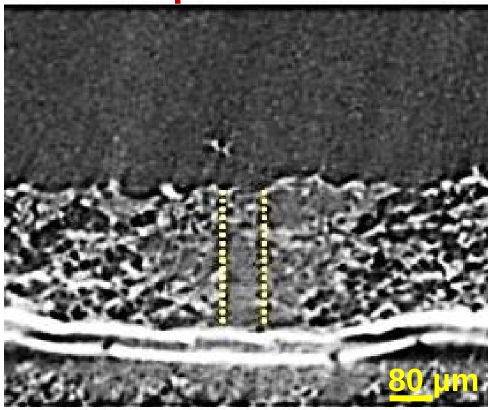

mechanic perforation

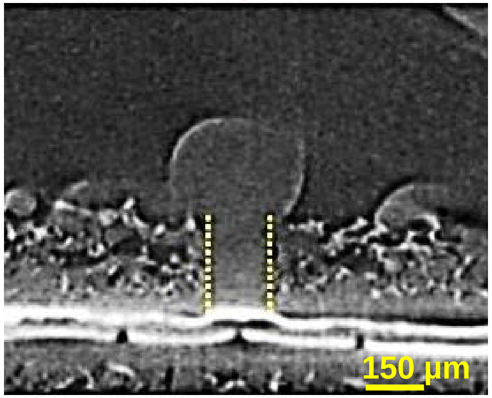

dynamic synchrotron radiography

Alexander Bauder
Robert Alink
Jan Haußmann
Joachim Scholta

J. Haußmann *et al.*,
Journal of Power Sources 239 (2013) 611

How to optimize water management in a PEM fuel cell?

Best case: 40% performance increase
Typical: 10-20% increase

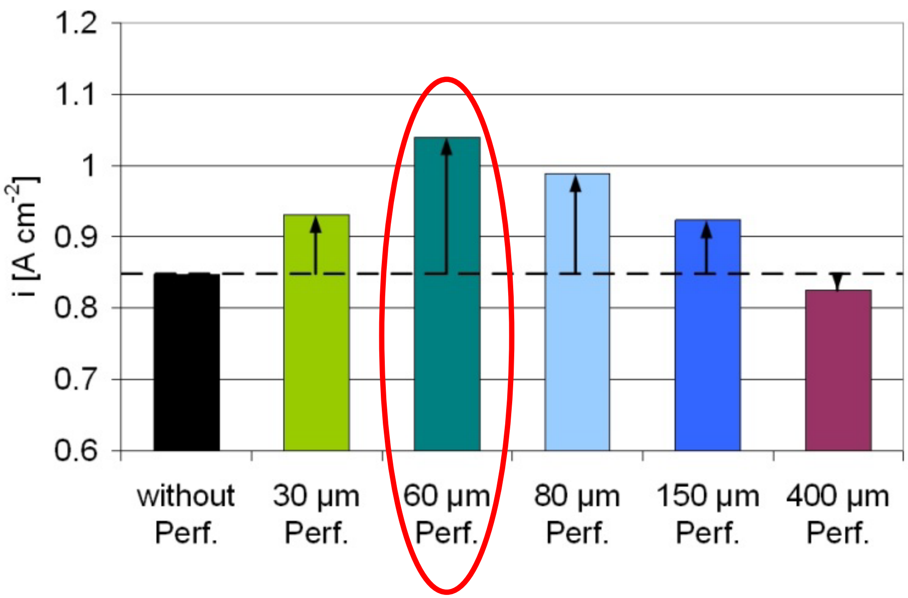

- *In-operando* visualization of water distribution

Diffusion dynamics revealed with D-H contrast

Photons: tailor-made microporosity improves water transport

Material now in production

→ **Optimized electrode design**

➡ **Improved performance under varying operation conditions**

Dual-mode imaging (X+N)

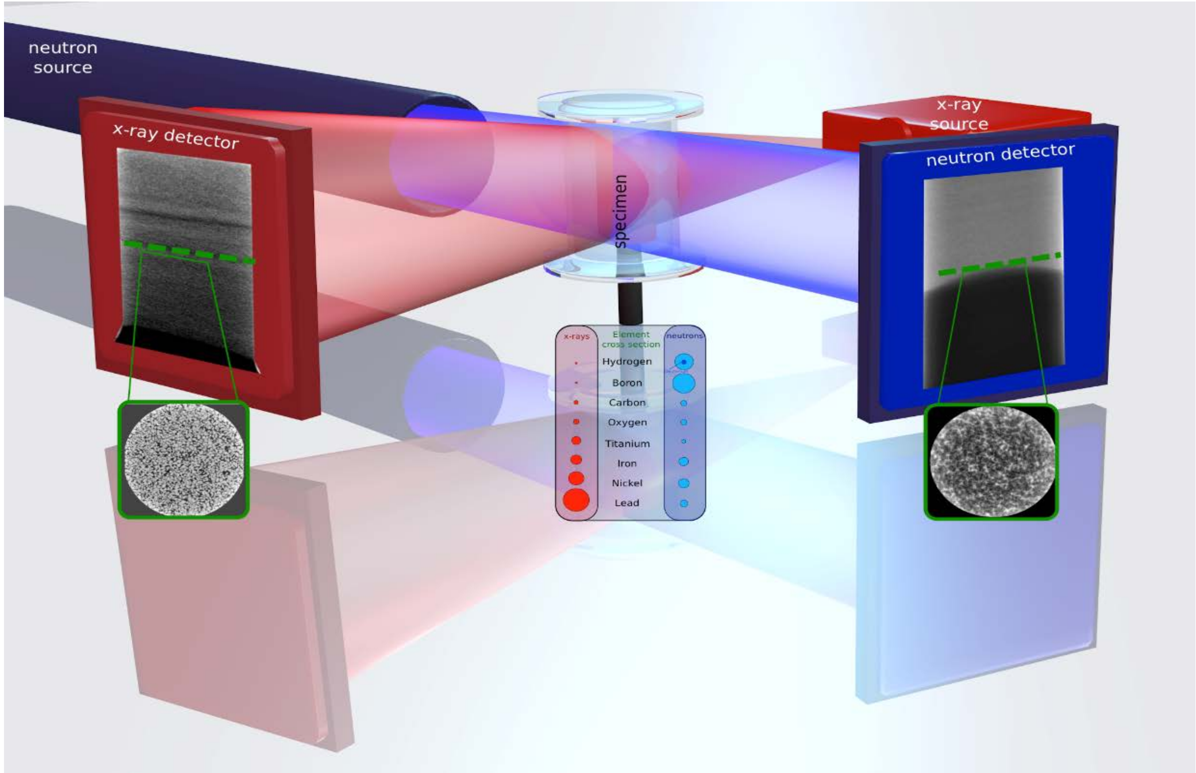

NeXT-Grenoble will be ILL's **first public Neutron and X-ray Tomograph**, born from a collaboration with the Université Grenoble Alpes (UGA) and Helmholtz-Zentrum Berlin (HZB):

Joint Research Unit

NI-Matters

It will be **a world-leading imaging instrument**, taking full advantage of the unique **flux of the ILL** (of particular importance in tomography), and employing state-of-the-art technical solutions to offer a **broad portfolio** of options and contrast mechanisms.

Tengattini, Alessandro, et al. "NeXT-Grenoble, the Neutron and X-ray tomograph in Grenoble." *Nuclear Instruments and Methods in Physics Research Section A* 968 (2020): 163939.

SiO_2 particles in water

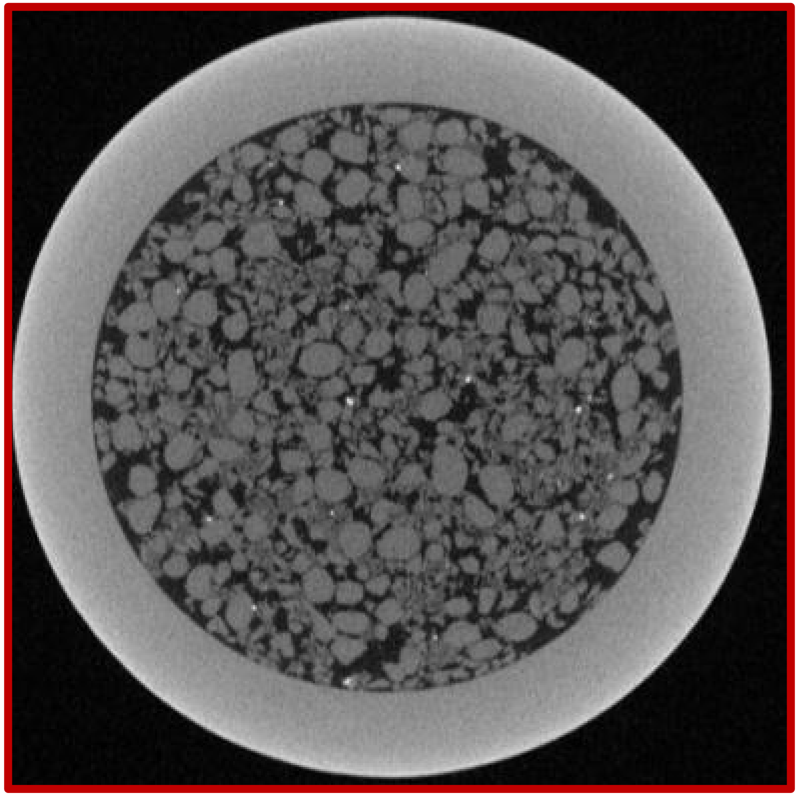

X-rays, 120 kV
Pixel size: 15 µm

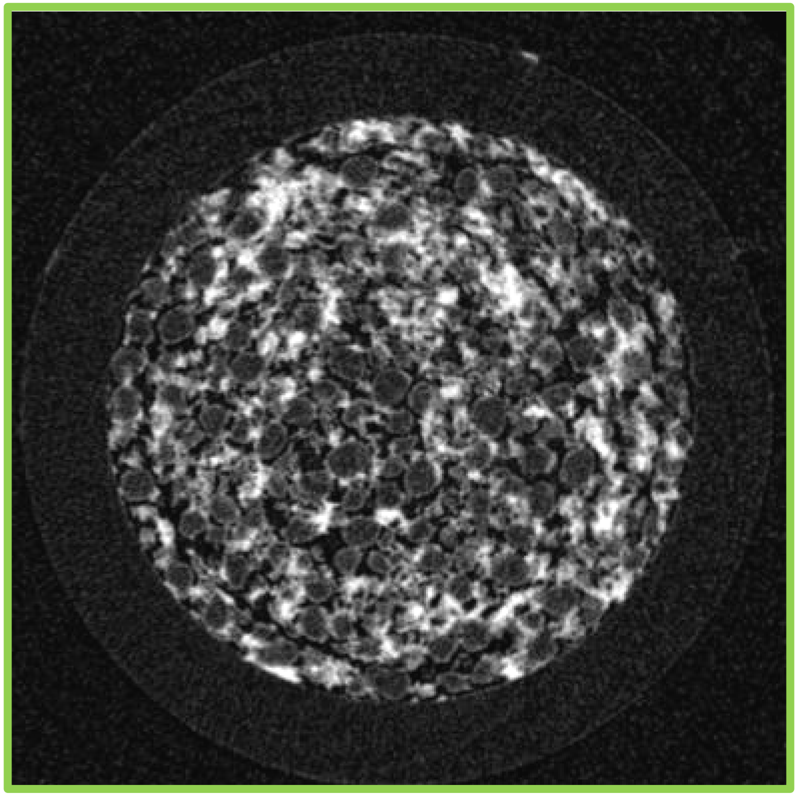

Cold neutrons

Pixel size: 13.5 µm (resolution: 30 µm)
Gadox 10 µm
Lens system: 200mm

Kim, Felix Hoyean. "Dual-Modality (Neutron And X-Ray) Imaging For Characterization Of Partially Saturated Granular Materials And Flow Through Porous Media." (2013).

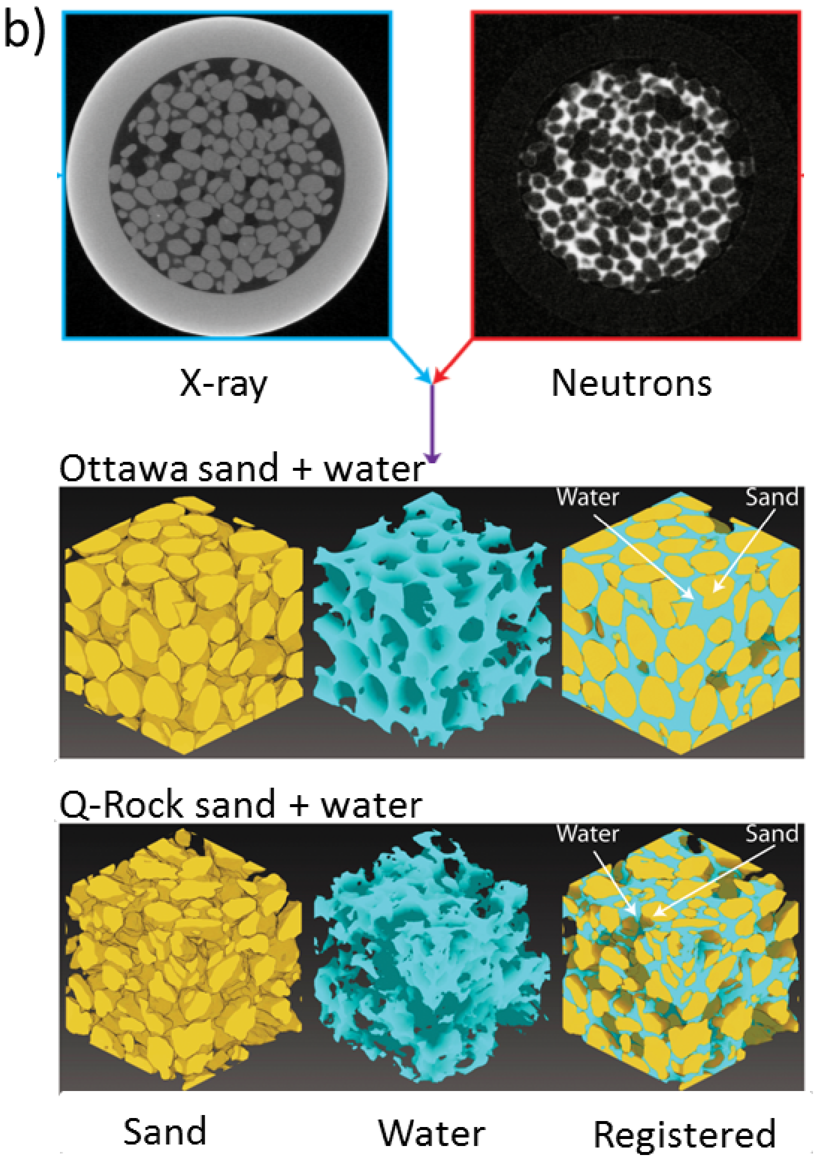

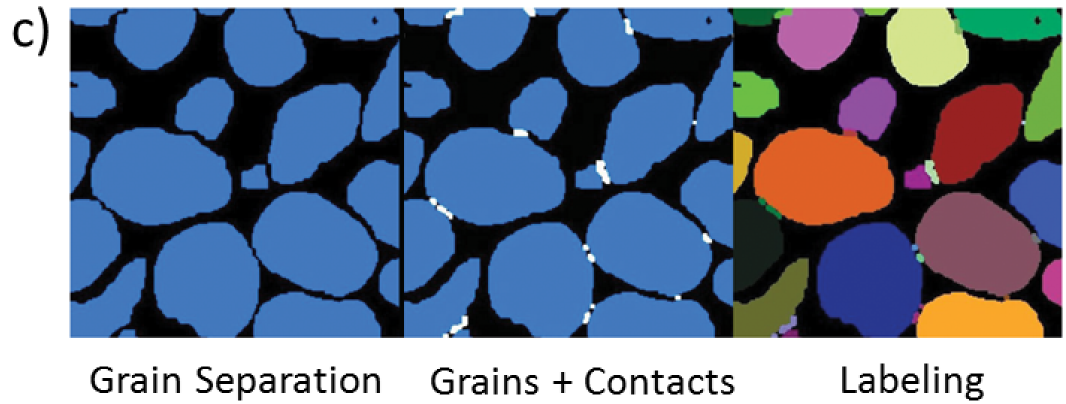

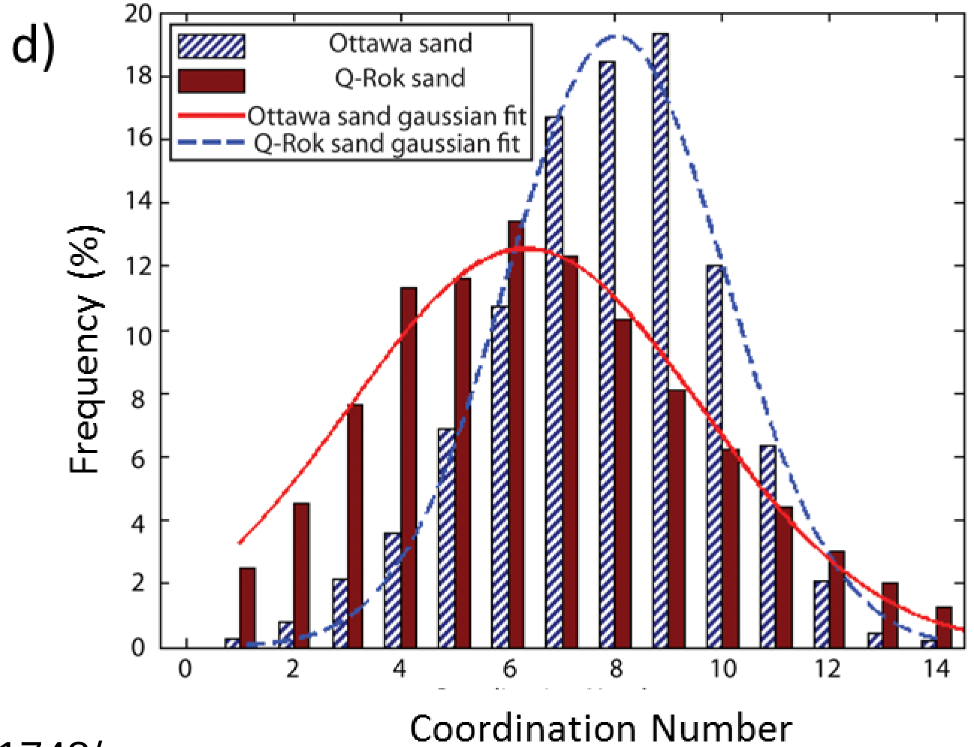

https://trace.tennessee.edu/utk_graddiss/1748/

A. Tengattini
L. Helfen
N. Lenoir

Ralf Ziesche
Paul Shearing

RF Ziesche, et al.
Nature communications 11.1 (2020): 1-11

How to characterize lithium intercalation in batteries?

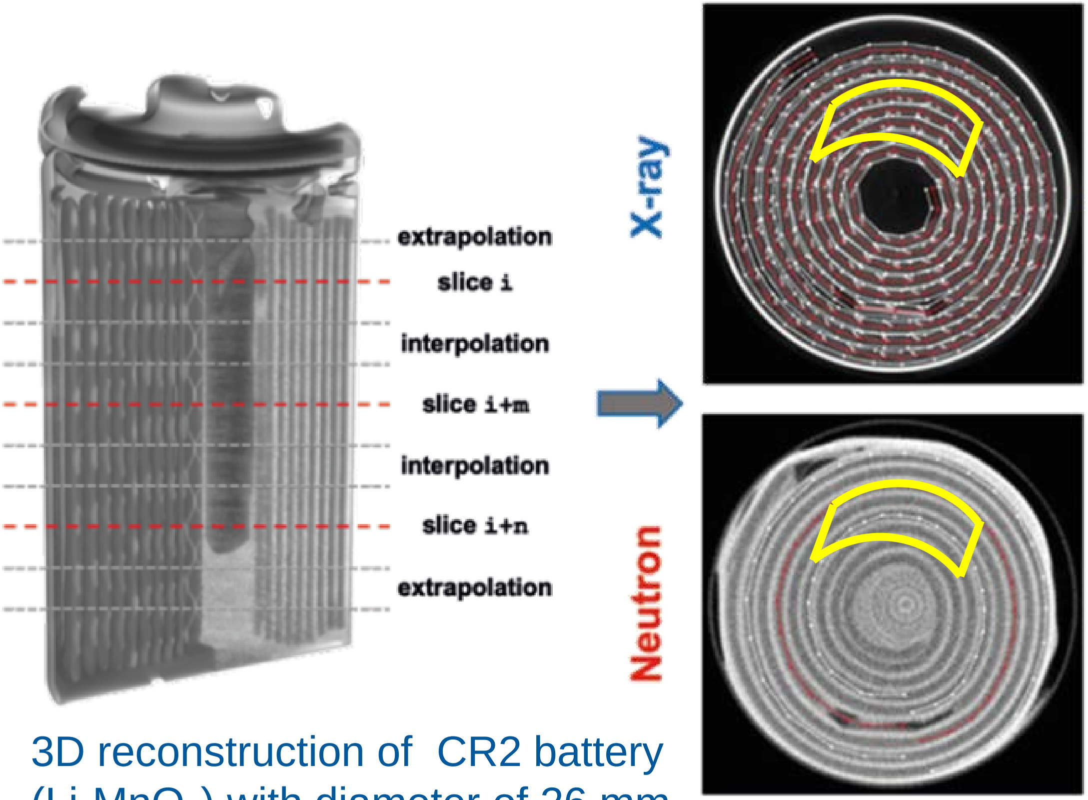

3D reconstruction of CR2 battery (Li_xMnO_2) with diameter of 26 mm.
(neutron tomography: pixel size: 13 µm, 600 projections /360°, time: 8 h)

- **3D+T investigation of batteries by dual-mode (X-ray/Neutron) tomography**

Virtual unrolling of the electrodes for different discharge times.

Lithium intercalation can be analyzed dynamically.

➔ Analysis of the dual-mode tomography data

➡ Temporally and spatially resolved tracking of lithium intercalation.

RF Ziesche, et al.
Nature communications 11.1 (2020): 1-11

A. Tengattini
L. Helfen
N. Lenoir
Ralf Ziesche
Paul Shearing

How to characterize lithium intercalation in batteries?

a

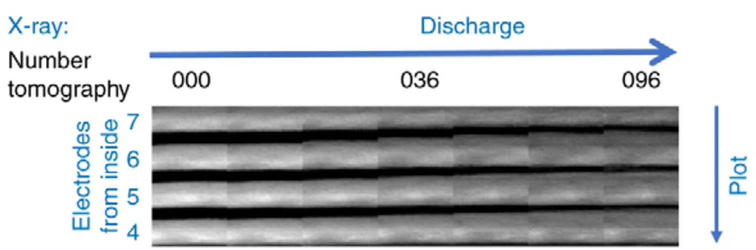

Capacity [|mAh|]	0	48	144	241	336	474	605
Breadth [µm]	389	414	431	442	467	486	495

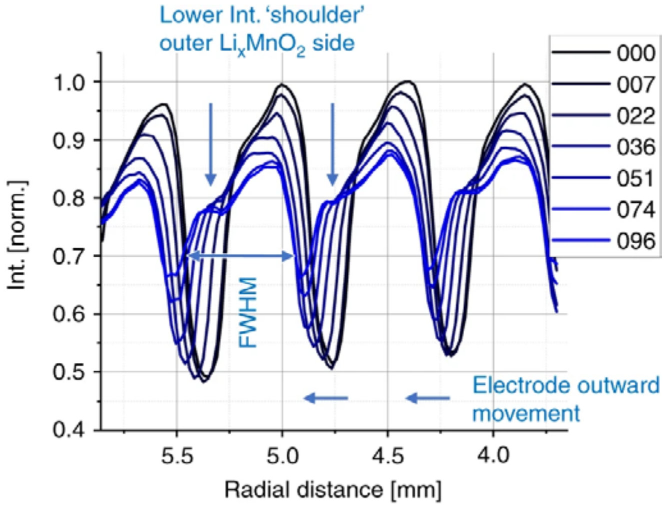

b

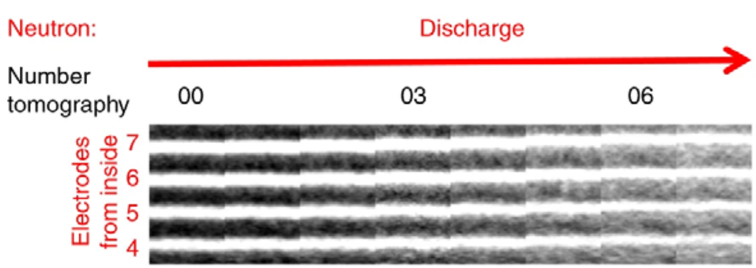

Capacity [|mAh|]	0	45	135	226	316	449	581	745
Breadth [µm]	386	392	423	427	453	461	488	501

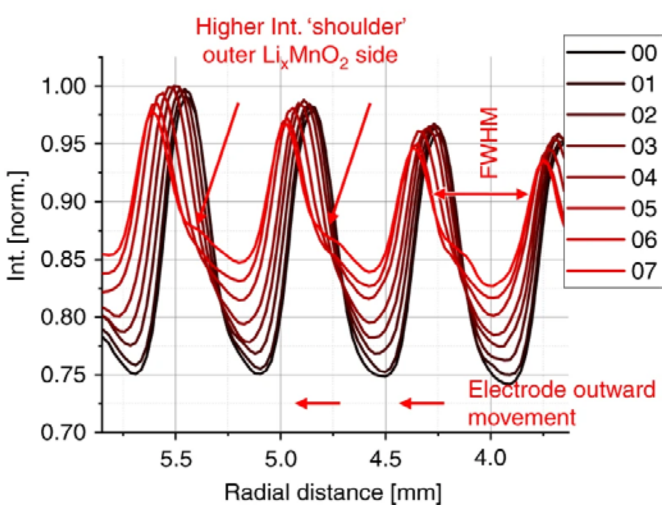

RF Ziesche, et al.
Nature communications 11.1 (2020): 1-11

A. Tengattini
L. Helfen
N. Lenoir

Ralf Ziesche
Paul Shearing

How to characterize lithium intercalation in batteries?

Electrode thickness dependence

a

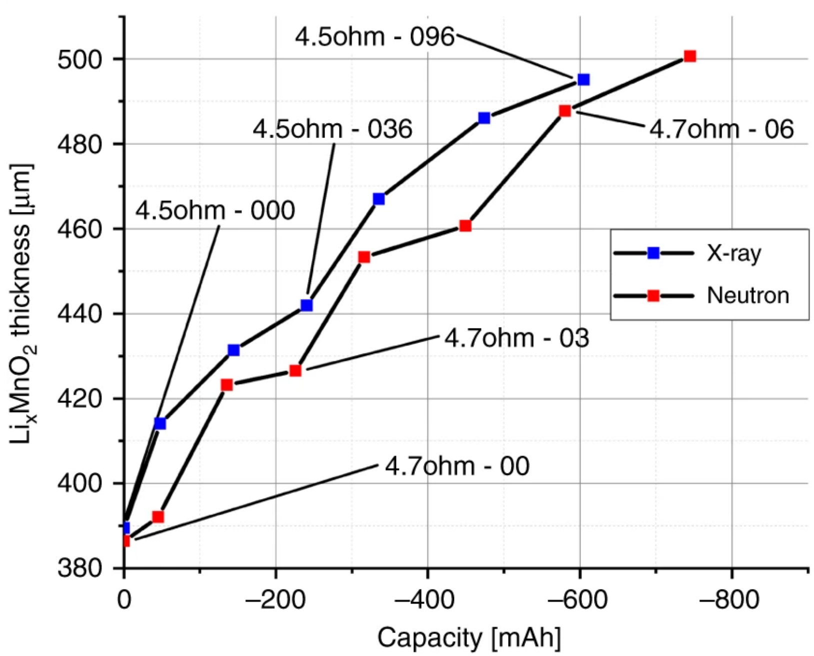

Lithium consumption

b

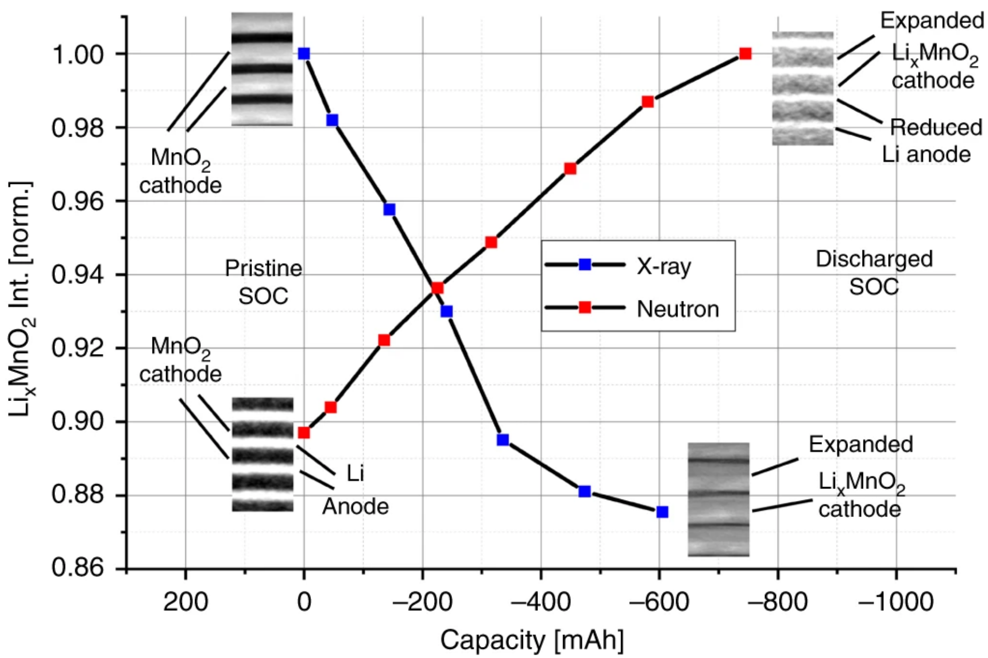

RF Ziesche, et al.
Nature communications 11.1 (2020): 1-11

A. Tengattini
L. Helfen
N. Lenoir
Ralf Ziesche
Paul Schering

How to characterize lithium intercalation in batteries?

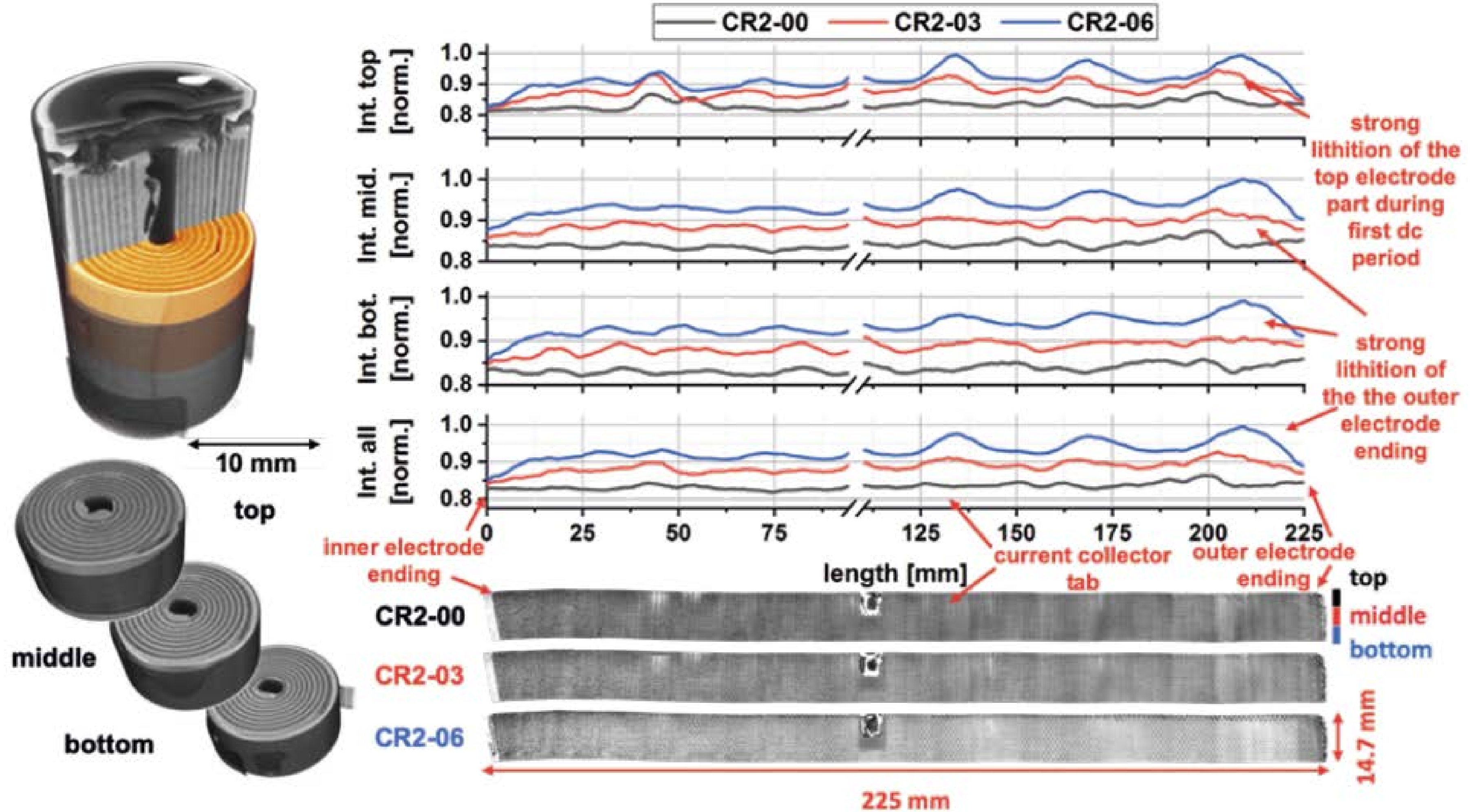

RF Ziesche, et al.
Journal of The Electrochemical Society 167.14 (2020): 140509

Ralf Ziesche
Paul Schering

How to characterize lithium diffusion in batteries?

4D Study of $SOCl_2$ Battery (pixel size: 8 µm, time step: 7.5 min)

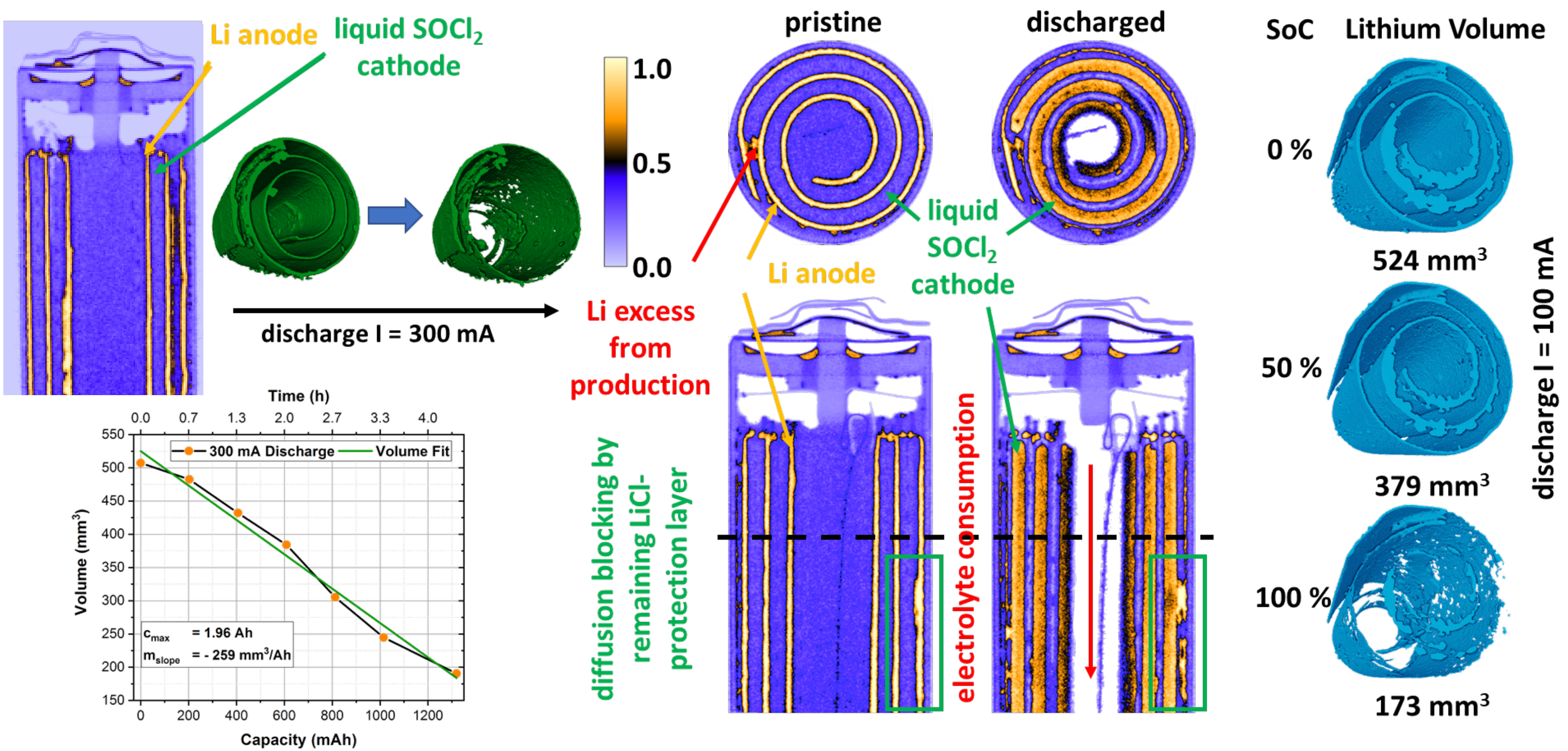

High temporal resolution

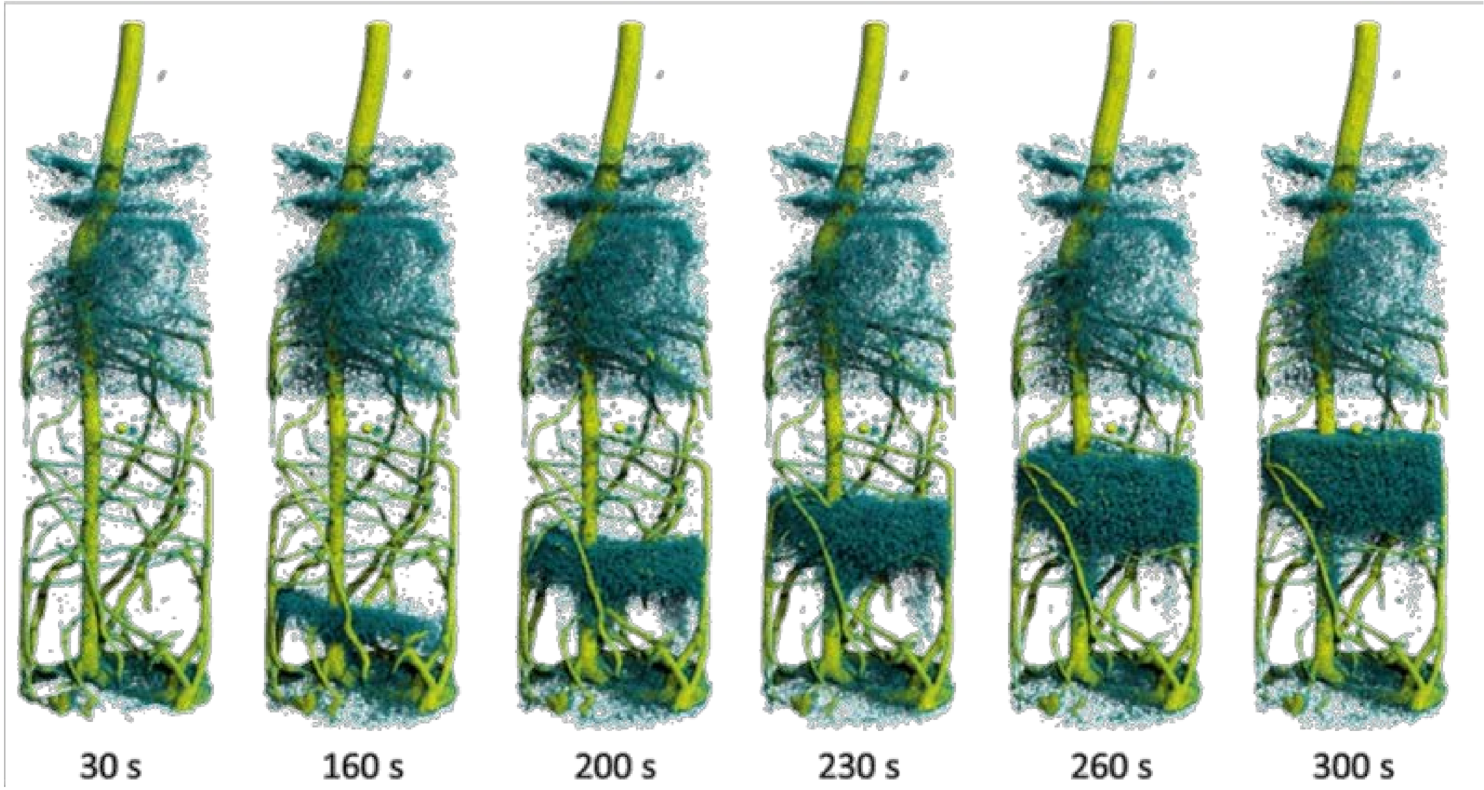

Ch. Tötzke, et al. *Scientific reports* 7.1 (2017): 6192.

Detector characterization

Exposure time readout

https://andor.oxinst.com/products/scmos-camera-series/neo-5-5-scmos

High-speed radiography

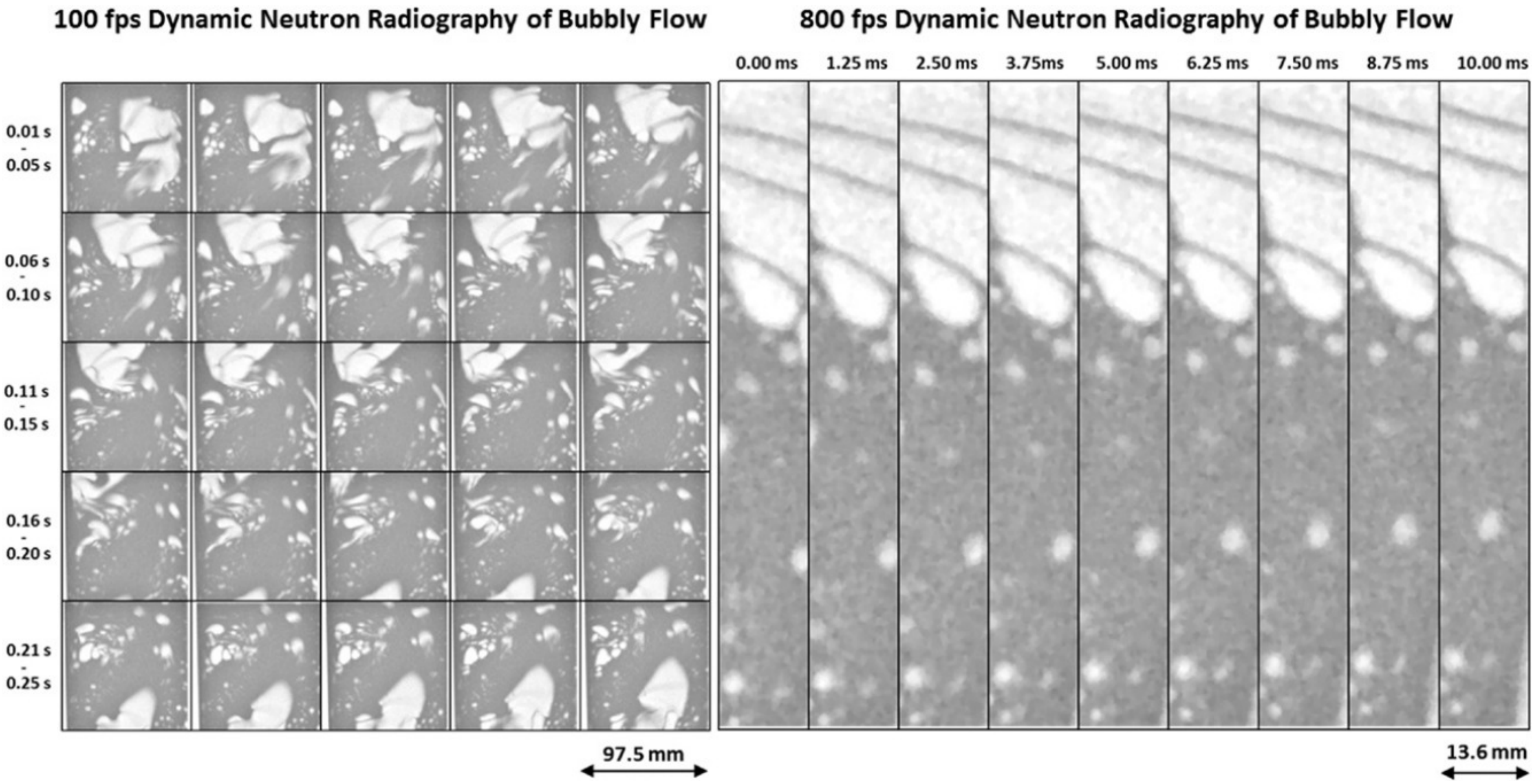

Robert Zboray, and Pavel Trtik.
"800 fps neutron radiography of air-water two-phase flow." *MethodsX* 5 (2018): 96-102.

High-speed radiography

Robert Zboray, and Pavel Trtik.
"800 fps neutron radiography of air-water two-phase flow." *MethodsX* 5 (2018): 96-102.

Plant's physiology

University of Potsdam
Christian Tötzke
Sascha E. Oswald

How to observe the water uptake in plant's root

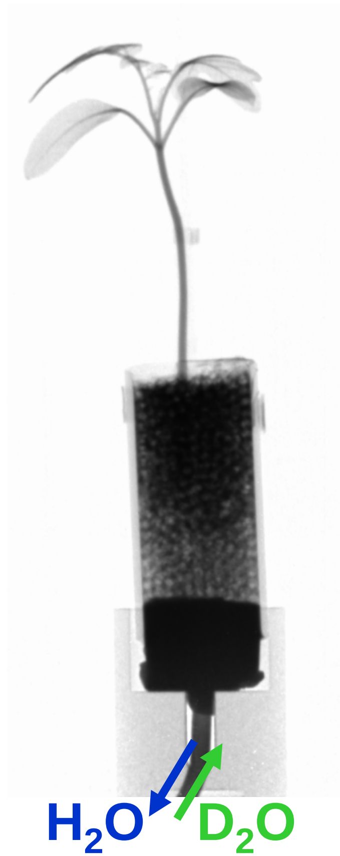

- *In-operando 3D* visualization of water distribution

Water uptake dynamics revealed with D-H contrast

Insights in the water uptake mechanisms in the root system

→ Observation of the dynamic processes in root system

➡ Learning about the root-soil interaction mechanisms

Plant's physiology

University of Potsdam
Christian Tötzke
Sascha E. Oswald

C. Tötzke, et al.
Scientific reports 7.1 (2017): 1-9.

How to observe the water uptake in plant's root

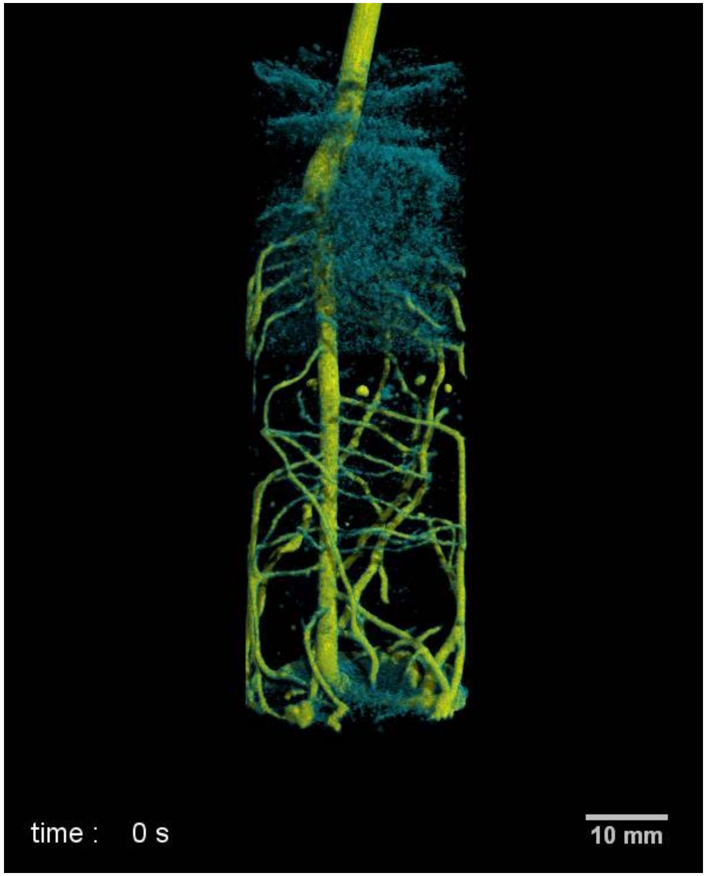

High-speed (on-the-fly) neutron tomography

resolution: 150 µm
exposure: 0.05 s
200 projections/180°

10 s / tomography

→ Observation of the dynamic processes in root system
➡ Learning about the root-soil interaction mechanisms

Plant's physiology

University of Potsdam
Christian Tötzke
Sascha E. Oswald

C. Tötzke, et al.
Scientific reports 7.1 (2017): 1-9.

How to observe the water uptake in plant's root

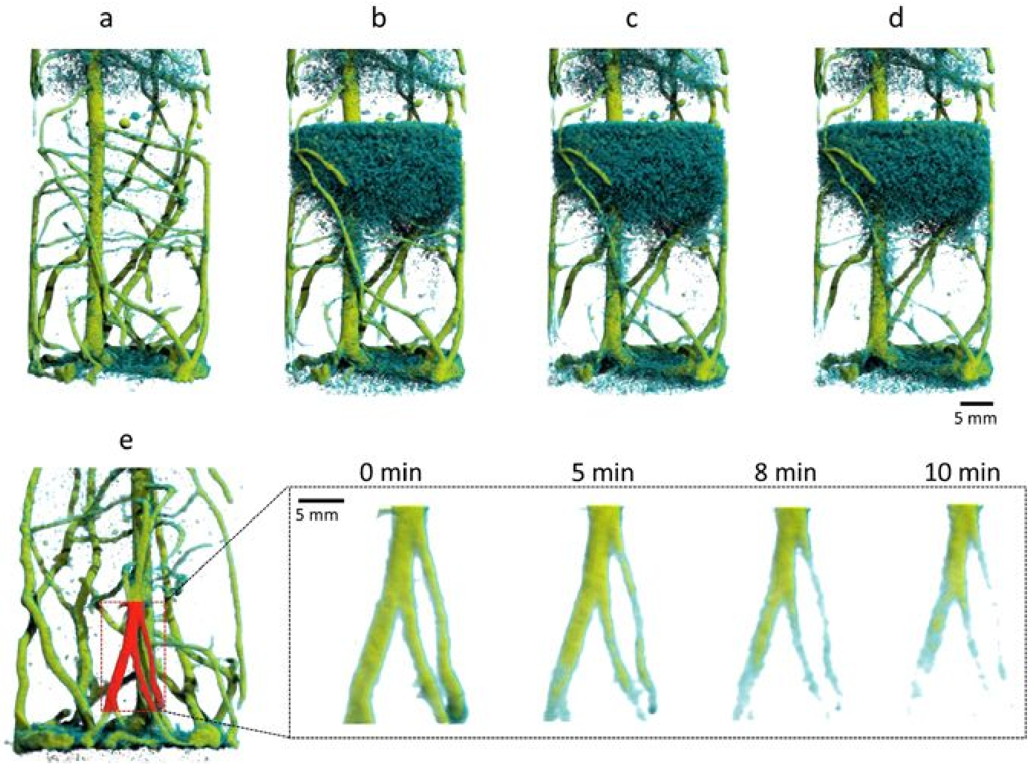

Time series of neutron tomograms at (a) 0 min; (b) 5 min; (c) 8 min and (d) 10 min after feeding D_2O.

High-speed (on-the-fly) neutron tomography

resolution: 150 µm
exposure: 0.05 s
200 projections/180°

10 s / tomography

Ch. Tötzke, et al. *Scientific reports* 7.1 (2017): 6192.

- → **Observation of the dynamic processes in root system**
- ➡ **Learning about the root-soil interaction mechanisms**

Plant's physiology

Recent experiments at ILL with 1.5 s / tomography

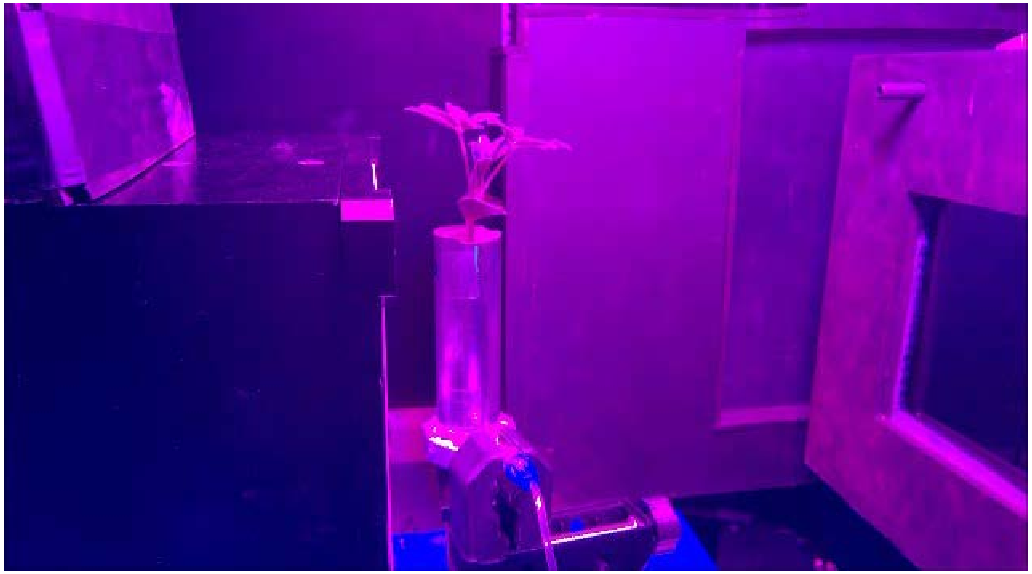

Problems:

- Speed of the rotation table
- Detector read-out time

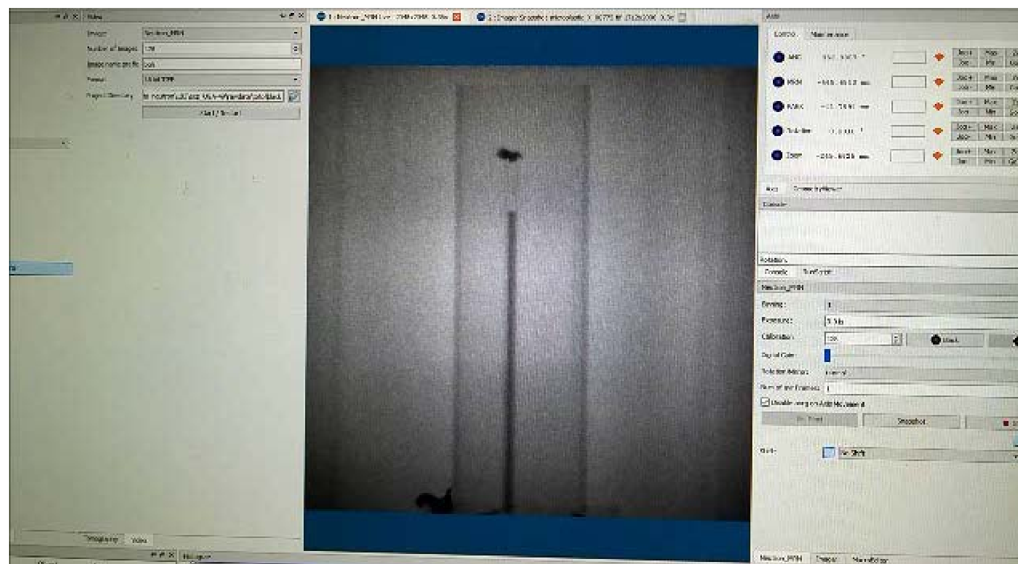

Large samples

Extreme samples




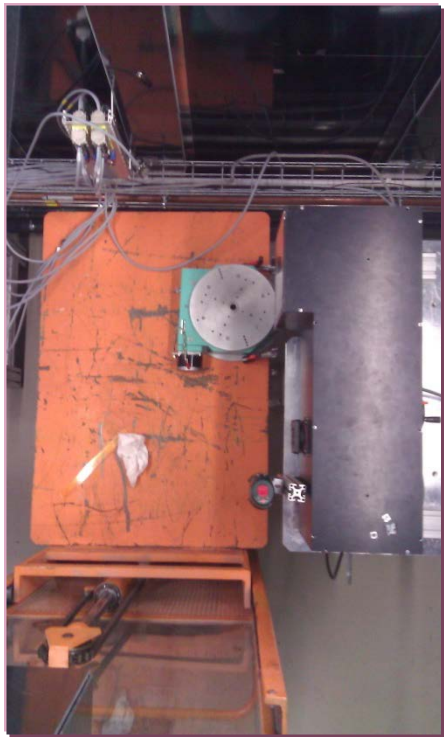

Extreme samples

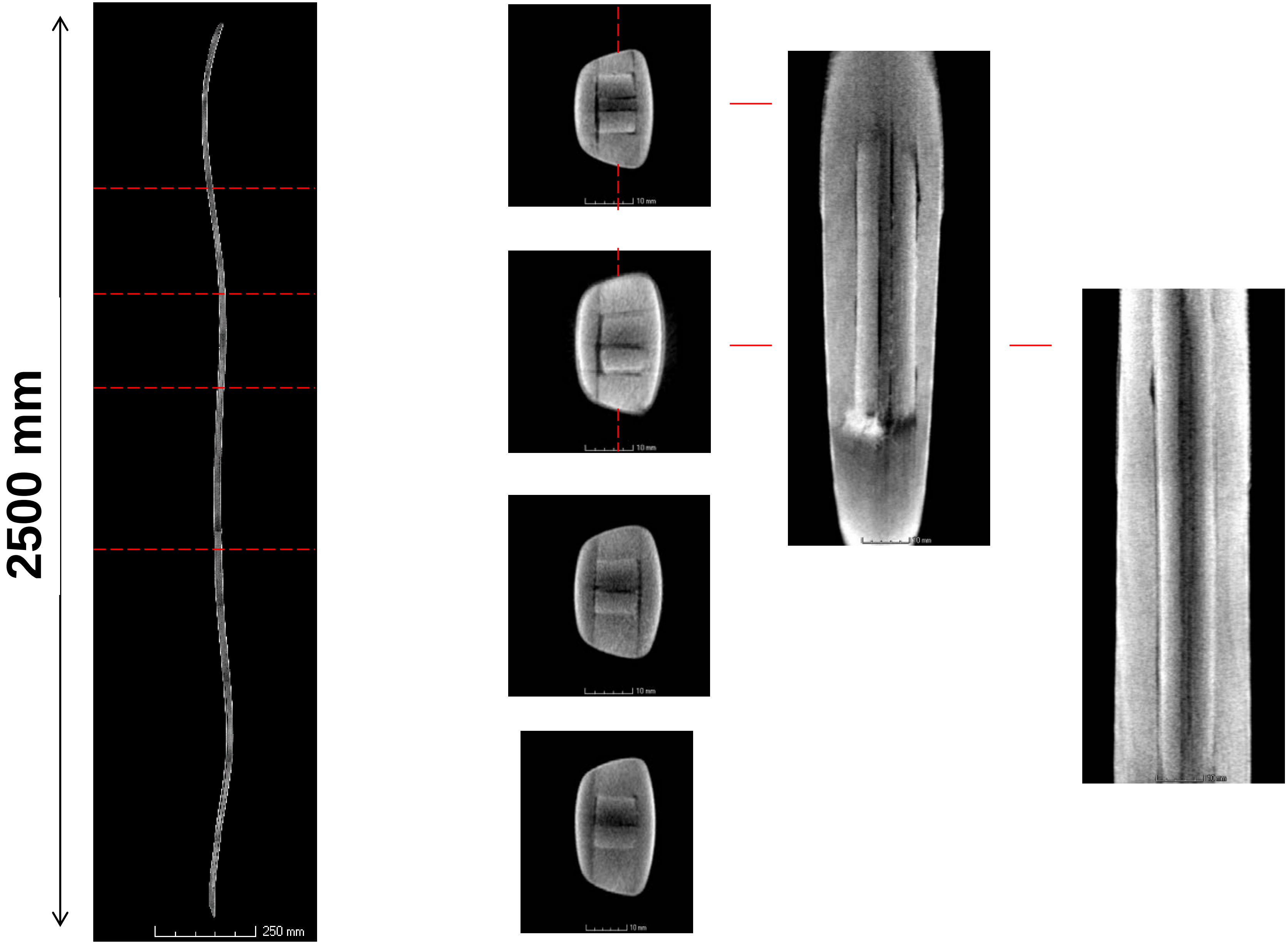

Shipwrecks

http://mapsontheweb.zoom-maps.com/image/64197912527

All routes lead to Rome: A map of Roman ports and trade routes

Attenuation Contrast

Lead blocks recovered near the UNESCO World Heritage Site Syracuse. Presumably I century A.D. (Roman Imperial Age).

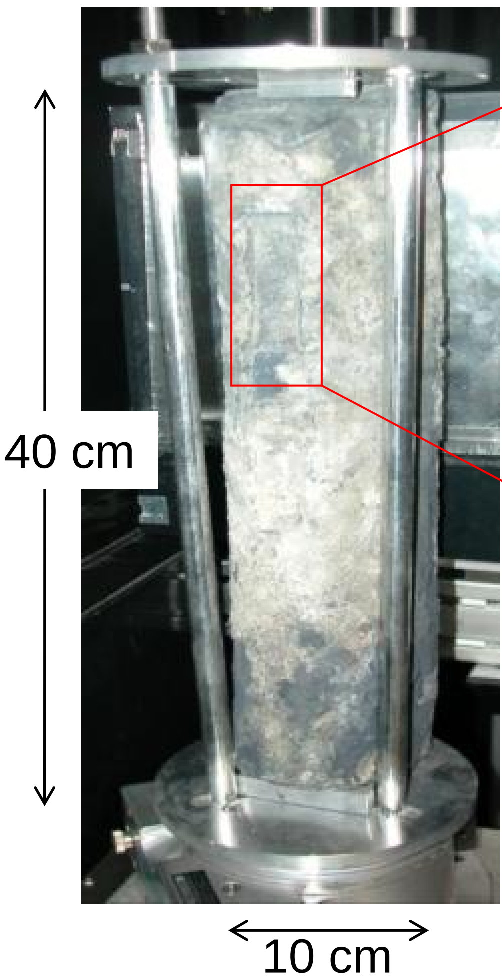

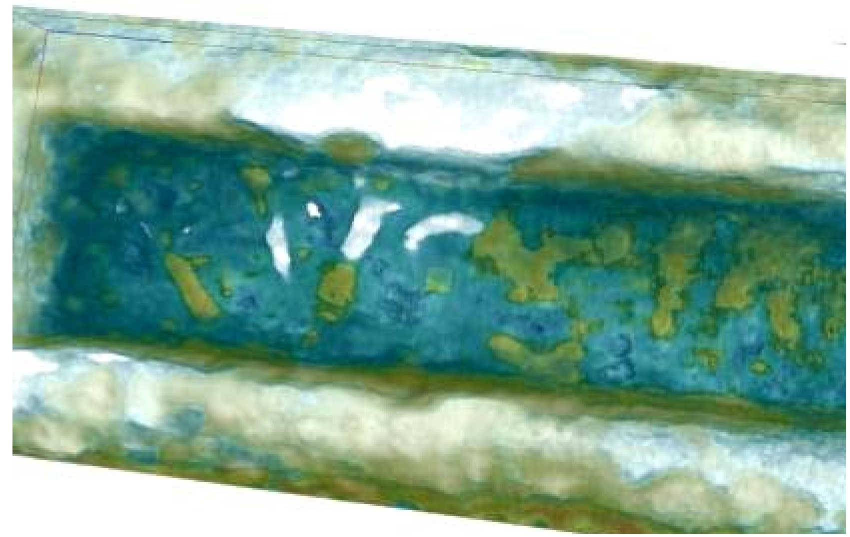

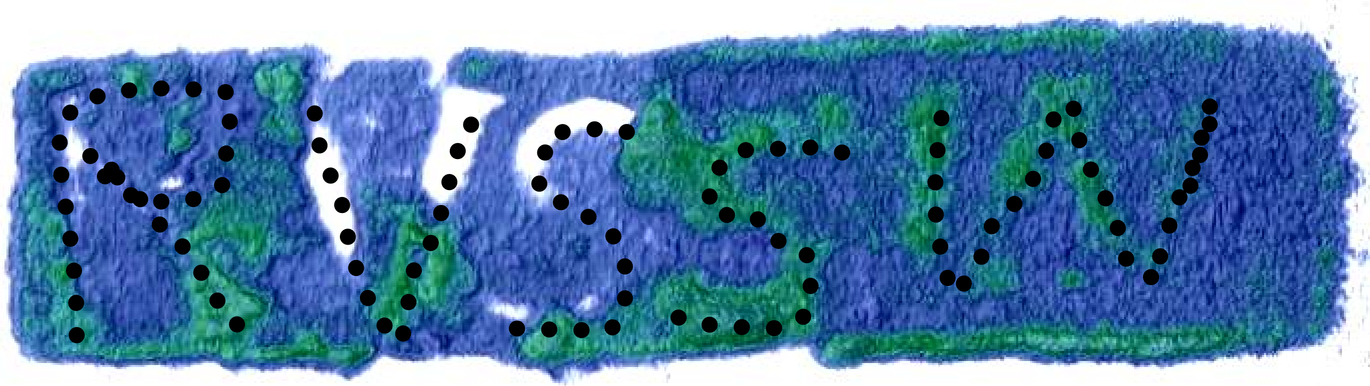

Triolo, R., et al. "Neutron tomography of ancient lead artefacts." *Analytical Methods* 6.7 (2014): 2390-2394.

Attenuation Contrast

Lead blocks recovered near the UNESCO World Heritage Site Syracuse. Presumably I century A.D. (Roman Imperial Age).

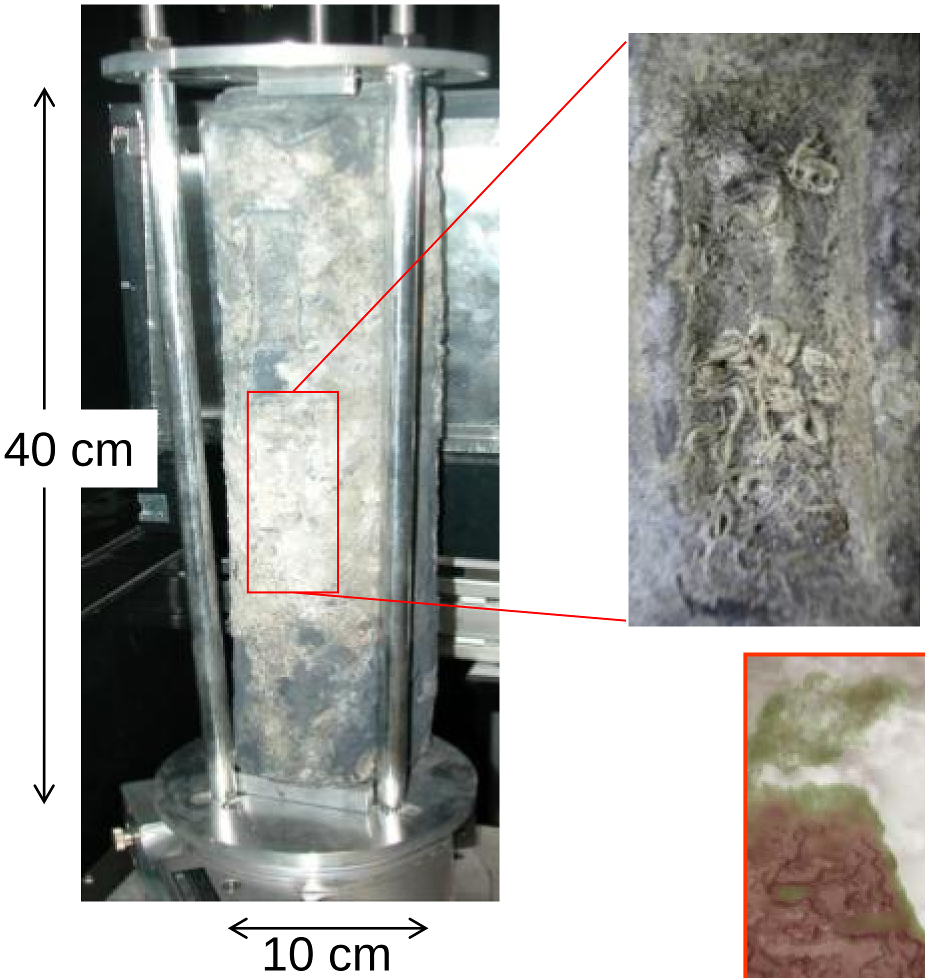

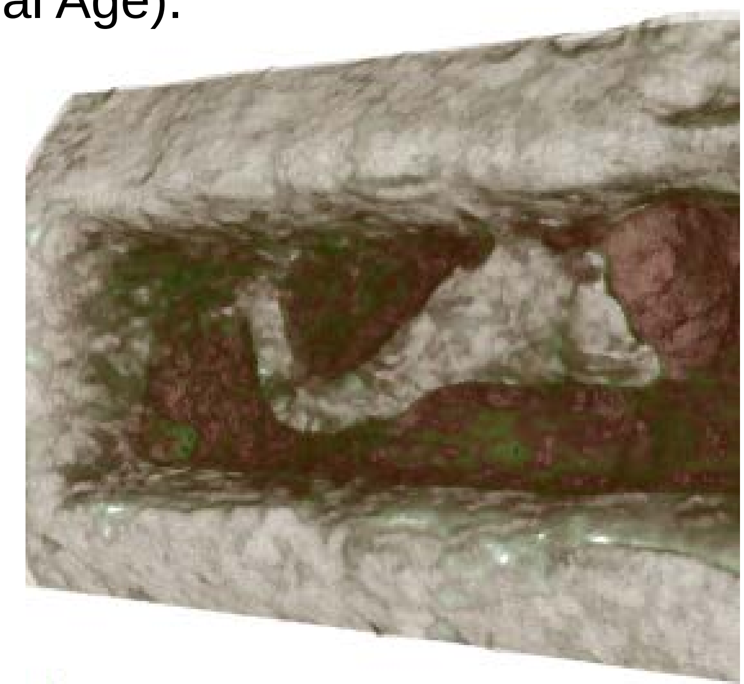

Triolo, R., et al. "Neutron tomography of ancient lead artefacts." *Analytical Methods* 6.7 (2014): 2390-2394.

Neutron tomography of bronze statues

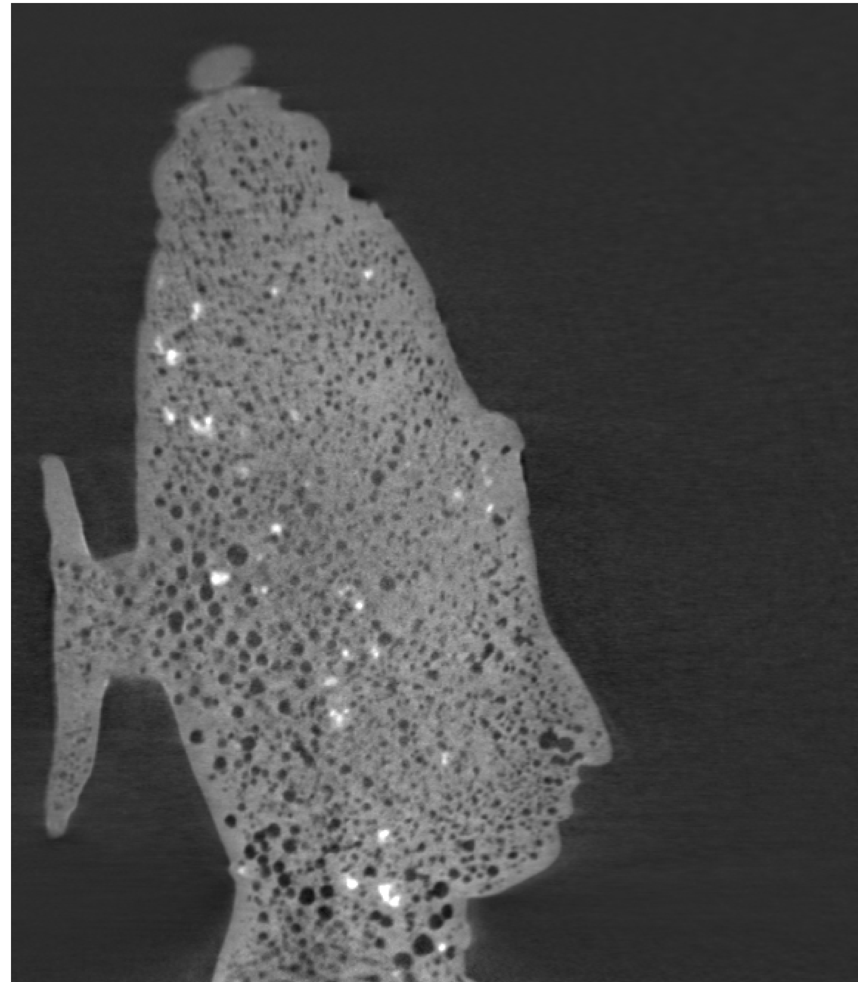

RIJKS MUSEUM amsterdam

https://indico.kfki.hu/event/518/contributions/1012/

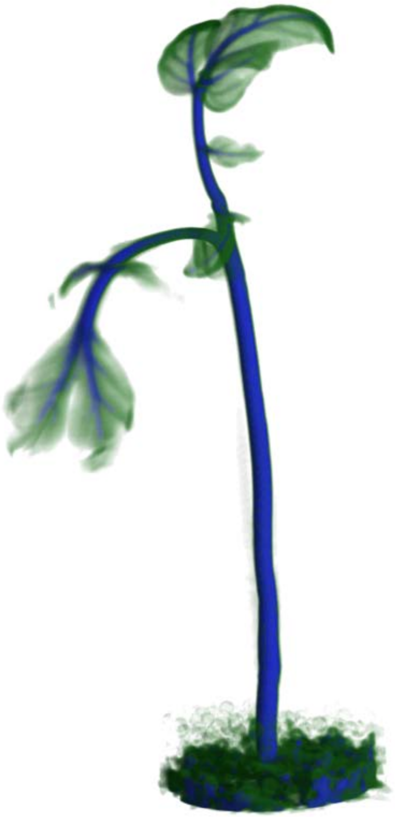

Thank you !